Estimation of Landscape-scale Fire Effects from Multi-temporal LiDAR

A Thesis

Presented in Partial Fulfillment of the Requirements for the

Degree of Master of Science

with a

Major in Geography

in the

College of Graduate Studies

University of Idaho

by

Travis Ryan McCarley

Major Professor: Crystal A. Kolden, Ph.D.

Committee Members: Andy T. Hudak, Ph.D.; Alistair M.S. Smith, Ph.D.

Department Administrator: Mickey E. Gunter, Ph.D.

July 2016

Authorization to Submit Thesis

This thesis of Travis Ryan McCarley, submitted for the degree of Master of Science with a Major in Geography and titled “Estimation of Landscape-scale Fire Effects from Multi-temporal LiDAR,” has been reviewed in final form. Permission, as indicated by the signatures and dates below, is now granted to submit final copies to the College of Graduate Studies for approval.

Major Professor: _____ Date: _____
Crystal A. Kolden, Ph.D.

Committee Members: _____ Date: _____
Andy T. Hudak, Ph.D.

_____ Date: _____
Alistair M.S. Smith, Ph.D.

Department Administrator: _____ Date: _____
Mickey E. Gunter, Ph.D.

Abstract

Measuring fire effects using remote sensing is critical to facilitating an ecological understanding of wildfire at the landscape scale, but questions remain regarding the relationship between spectral changes caused by fire, forest biometrics, and pre-fire agents of change. This thesis addresses these questions by (1) comparing structural forest changes estimated from Light Detection and Ranging (LiDAR) with spectral changes captured by Landsat, and (2) exploring the effects of an antecedent mountain pine beetle (*Dendroctonus ponderosae*; MPB) outbreak and forest treatments on subsequent fire effects. The strongest correlations were observed between LiDAR-estimated change in canopy cover (dCC) and spectral indices incorporating the shortwave infrared band. Compared to areas experiencing no pre-fire agent of change, dCC was higher in pre-fire MPB and lower in pre-fire treatments. These results demonstrate the utility of multi-temporal LiDAR to measure fire effects and the importance of antecedent MPB and forest treatments on subsequent wildfire severity.

Acknowledgements

I would like to acknowledge those who influenced this work and helped make this thesis possible. Thank you foremost to the committee, Crystal Kolden, Andy Hudak, and Alistair Smith, for guidance and direction. Nicole Vaillant provided invaluable insights and an opportunity to see the Pole Creek burn area in person. Conversations with University of Idaho colleges helped shape some of the methods and fill certain knowledge gaps. Credit goes to Arjan Meddens, Steven Radil, and all the member of the Pyrogeography lab, Tyler Bleeker, Vincent Jansen, Aaron Sparks, and Devin Yeatman, whom with I was fortunate to share an office.

This research was partially funded by the Western Wildland Threat Assessment Center under JVA #13-JV-11261900-072.

Table of Contents

List of Figures

List of Tables

Thesis Introduction

Mapping wildfire effects is critically important. Following a wildfire, managers and scientists seek to understand rehabilitation needs (Hessburg et al., 2015; Turner, Hargrove, Gardner, & Romme, 1994) and predict trends in ecological recovery (Cansler & Mckenzie, 2014; Eidenshink et al., 2007; Miller, Safford, Crimmins, & Thode, 2009). Secondary fire effects, such as flooding and erosion, provide an urgent need to identify at-risk areas using these maps (Moody, Martin, Haire, & Kinner, 2008; Robichaud, Lewis, Brown, & Ashmun, 2009). And at the broader scale, fire effects mapping is used to understand how climate change is affecting forest carbon cycling (Conard et al., 2002; Goetz, Mack, Gurney, Randerson, & Houghton, 2007; Hicke et al., 2003; Kashian, Romme, Tinker, Turner, & Ryan, 2006; Romme et al., 2011). All of these tasks are vitally important and likely to become more so as climatic shifts toward larger, more extreme wildfires occur (Barbero, Abatzoglou, Larkin, Kolden, & Stocks, 2015; Littell, McKenzie, Peterson, & Westerling, 2009; Westerling, Hidalgo, Cayan, & Swetnam, 2006).

Remote sensing is the primary tool allowing managers and scientists to understand fire effects at the landscape scale (Lentile et al., 2006). Early attempts to classify fire effects using passive sensors (i.e., Landsat) demonstrated that Landsat Thematic Mapper (TM) band 7 (shortwave infrared: 2.08-2.35µm) is particularly sensitive to lack of vegetation and/or moisture associated with a fire (Jakubauskas, Lulla, & Mausel, 1990; White, Ryan, Key, & Running, 1996). This led to the development of the Normalized Burn Ratio (NBR; Lopez-Garcia & Caselles, 1991), which was used for burned area delineation, and delta NBR (dNBR; Key & Benson, 2006) and Relative delta NBR (RdNBR; Miller & Thode, 2007) to measure variations in fire effects. These indices have become ubiquitous in fire ecology research (e.g., Eidenshink et al., 2007; French et al., 2008; Lentile et al., 2006; Zhu, Key, Ohlen, & Benson, 2006). However, there are widespread concerns about the ability for these indices to accurately differentiate burned and unburned pixels (Kolden, Lutz, Key, Kane, &

van Wagtendonk, 2012; Sparks et al., 2015) and delineate severity classes without adequate ground observations (Kolden, Smith, & Abatzoglou, 2015). Furthermore, without specific correlation to any biometric measure of severity, many researchers are finding spectral indices alone to be suboptimal metrics (Kolden et al., 2015; Morgan et al., 2014; Roy, Boschetti, & Smith, 2013; Roy, Boschetti, & Trigg, 2006; Smith et al., 2016).

Forest structural attributes derived from Light Detection and Ranging (LiDAR) data may provide a viable alternative to spectral indices, by providing an estimate of changes in vegetation structure associated with a wildfire (Smith et al., 2014). LiDAR is an active remote sensing method that is growing in prominence among natural resource managers and scientists (Hudak, Evans, & Smith, 2009). Sensors are now ground-, air-, and space-based, although airborne LiDAR is particularly well suited to landscape scale studies in forested ecosystems. Measurements are made by calculating the angle and distance between the sensor and target using a global positioning system and the elapsed time for the light to make the round-trip from the sensor to the target and back. LiDAR can estimate structural attributes, such as height, cover, height distribution of outer canopy surfaces, vertical distribution of canopy material, volume, biomass, and gap size (Hudak et al., 2009; Kane et al., 2013; Lefsky, Cohen, Parker, & Harding, 2002). LiDAR has also been successfully used to map bark beetle effects (Bater, Wulder, White, & Coops, 2010; Bright, Hicke, & Hudak, 2012) and fuel loads (Andersen, McGaughey, & Reutebuch, 2005; Seielstad & Queen, 2003). While greater attention has been paid to characterizing fire fuel structure, only a few studies have used LiDAR to quantify post-fire effects (Bishop, Dietterick, White, & Mastin, 2014; Kane et al., 2013, 2014; Reddy et al., 2015; Wang & Glenn, 2009; Wulder et al., 2009) and even fewer have used pre- and post-fire LiDAR acquisitions (Bishop et al., 2014; Reddy et al., 2015; Wang & Glenn, 2009; Wulder et al., 2009).

Repeat acquisition of LiDAR in 2009 and 2013, spatially coincident with the 2012 Pole Creek fire in central Oregon along the eastern Cascades, provided a unique opportunity to

demonstrate the utility of multi-temporal LiDAR to estimate fire effects. This thesis utilizes these data to explore the relationship between multi-temporal LiDAR and conventional spectral remote sensing of fire effects. It also exhibits the application of multi-temporal LiDAR to provide novel insights on the effect pre-fire agents of change have on subsequent fire effects. Each of the chapters in this paper corresponds with an objective.

The goal of chapter one was to explore the relationships of spectral indices calculated from Landsat imagery and changes in forest structure estimated from multi-temporal LiDAR. A secondary theme of this chapter was the use of simultaneous autoregression, a spatially weighted regression model, to improve performance by providing a proxy for other variables (i.e., geomorphic or climatic process) not in the model (Kissling & Carl, 2007; Prichard & Kennedy, 2014; Wimberly, Cochrane, Baer, & Pabst, 2009). This study included 21 spectral indices and 24 LiDAR metrics as candidate variables, eliminating poorly correlated combinations, resulting in 63 viable models to evaluate. Both ordinary least squares regression and simultaneous autoregression were applied to these pairs, although model evaluation using Akaike's Information Criterion (AIC; Akaike, 1974) showed the spatial models were superior in each case. LiDAR-estimated change in canopy cover (dCC) and a multi-temporal ratio of Landsat's second shortwave infrared and near infrared bands (d74) had the highest correlation (psedo-r^2 = 0.86), followed by dNBR and dCC (psedo-r^2 = 0.85). Correlation with LiDAR metrics closer to the ground was not well detected by spectral indices. Like past studies, it was observed that Landsat band 7 is most sensitive to fire effects (Key & Benson, 2006; Miller & Yool, 2002; van Wagtendonk, Root, & Key, 2004; White et al., 1996); however, correlation with a substantive severity metric (i.e., dCC) was also demonstrated. This work sets the stage for future opportunities to calibrate spectral indices to structural measures of change at larger scales.

The goal of chapter two was to explore the impact of pre-fire agents of change, in this case mountain pine beetle (*Dendroctonus ponderosae*; MPB) and timber harvest, on subsequent fire-

caused change in canopy cover, estimated by multi-temporal LiDAR (dCC). This chapter used MPB estimates of mortality occurring 6-12 years prior to the fire and locations for timber harvest and hazardous fuel reduction treatments conducted by the Deschutes National Forest between 1971 and 2009. Areas being affected by all possible combinations of forest agents were identified and evaluated, including: (1) MPB followed by wildfire (MPB/Fire), (2) harvest followed by wildfire (HARV/Fire), (3) a combination of forest harvest and MPB followed by fire (HARV/MPB/Fire), (4) wildfire having not been proceeded by either MPB or harvest (Fire-only), (5) MPB, (6) HARV, (7) HARV/MPB, and (8) no pre-fire agent (No Agent/No Fire). Pre-fire MPB intensity, harvest treatment type, and harvest treatment age were also examined. Results indicate that MPB/Fire areas had higher average dCC than Fire-only, and that dCC increased with pre-fire MPB-mortality. Timber harvest, on the other hand, appeared to reduce dCC compared to Fire-only. A relationship was observed with dCC and treatment age, with the most recent treatments experiencing the lowest dCC. Treatment type did not appear to be as important. This method of measuring fire effects across the landscape is a noteworthy improvement over studies limited to post-fire data only, as well as those using dNBR or RdNBR without any kind of biometric validation. The findings regarding harvest treatment areas generally agree with previous research (e.g., Moghaddas & Craggs, 2007; Prichard, Peterson, & Jacobson, 2010; Ritchie, Skinner, & Hamilton, 2007; Safford, Schmidt, & Carlson, 2009; Safford, Stevens, Merriam, Meyer, & Latimer, 2012; Wimberly et al., 2009). However, there is still significant uncertainty regarding the impact of MPB (Hicke, Johnson, Hayes, & Preisler, 2012) and the finding of increased burn severity contradicts recent studies conducted in the same area (Agne, Woolley, & Fitzgerald, 2016; Meigs, Zald, Campbell, Keeton, & Kennedy, 2016). While additional research is needed on the topic of pre-fire agents of change, the use of multi-temporal LiDAR demonstrates considerable promise in the field of fire ecology.

Chapter 1: Multi-temporal LiDAR and Landsat Quantification of Fire Induced Changes to Forest Structure

T. Ryan McCarley, Crystal A. Kolden, Nicole M. Vaillant, Andrew T. Hudak, Alistair M.S. Smith, Brian M. Wing, Bryce Kellogg, Jason Kreitler

In review for *Remote Sensing of Environment*

Abstract

Measuring post-fire effects using remote sensing is critical to an ecological understanding of wildfire at the landscape scale. Predominantly this is accomplished with multi-spectral reflectance data, which provide frequent, synoptic observations of spectral changes in the top-most Earth surface (often forest canopy), and ground-based field sample plots, which are usually limited to post-fire observations. This study quantifies wildfire burn severity by comparing forest changes in biomass and structure derived from multi-temporal Light Detection and Ranging (LiDAR) acquisitions with spectral changes captured by the Landsat Thematic Mapper (TM) and the Operational Land Imager (OLI) sensors. Data acquired before and after the 2012 Pole Creek Fire in central Oregon along the eastern Cascade Mountains were utilized to assess the potential for spectral indices to predict forest structural changes. The strongest correlations were observed using a LiDAR-derived estimate of change in canopy cover. A simple ratio of shortwave infrared and near infrared light (d74), the delta Normalized Burn Ratio (dNBR), and the delta Normalized Vegetation Index (dNDVI) were the top three predictor indices (psedo-$r^2 > 0.84$, $p < 0.01$). For the most part, correlation between percentage of LiDAR returns in forest strata and spectral indices increased with strata height. Structural measurements made closer to the ground and statistical measures of the point cloud such as mean, standard deviation, and skewness were not well correlated. Additionally, the results indicated that the presence of pre-fire mountain pine beetle mortality negatively affected the performance of the

Relative delta Normalized Burn Ratio (RdNBR) by producing significant outliers at the edge of the disturbance where pre-fire NBR was near zero. This study demonstrates that spectral indices such as d74, dNBR, and dNDVI are most sensitive to wildfire-caused structural changes akin to reduction in canopy cover and less sensitive to fire effects near the surface in a forested ecosystem. These results establish the utility of spectral methods to predict changes in canopy structure under certain fire regimes, as multi-temporal LiDAR is not available everywhere.

Keywords: wildfire, eastern Cascades, dNBR, RdNBR, canopy cover, mountain pine beetle

1. Introduction

Remote sensing imagery plays a critical role in allowing managers and scientists to assess fire effects across landscapes (Lentile et al., 2006). Accurate detection of wildfire severity is required to evaluate potential ecological rehabilitation needs (Hessburg et al., 2015; Turner et al., 1994), mitigate secondary fire effects (e.g., flooding and erosion) (Moody et al., 2008; Robichaud et al., 2009), monitor anomalies and trends in ecological recovery (Cansler & Mckenzie, 2014; Eidenshink et al., 2007; Miller, Safford, et al., 2009), and quantify carbon balance (Meigs, Donato, Campbell, Martin, & Law, 2009; Randerson, Chen, van der Werf, Rogers, & Morton, 2012). In light of increasing frequency and size of wildfires under climate change (Barbero et al., 2015; Westerling et al., 2006) and the inherent inter-annual variability of fire seasons (Moritz et al., 2012), the ability to accurately quantify long-term carbon stocks is necessary for understanding biosphere-atmosphere feedbacks (Li, Bond-Lamberty, & Levis, 2014). The long-term impacts of fire severity on forest carbon stocks and processes have been characterized by only a few studies including those focused on recovery in high latitude ecosystems (Conard et al., 2002; Goetz et al., 2007; Hicke et al., 2003) and recovery following the Yellowstone 1988 fires (Kashian et al., 2006; Romme et al., 2011). While considerable advances have been made in relating observed changes associated with fire effects to remote sensing

data (Disney et al., 2011; Lentile et al., 2006; Smith et al., 2016), there are still knowledge gaps and several known sources of uncertainty that can lead to extensive errors when applied to regional assessments (Kolden et al., 2015; Roy et al., 2006; Smith et al., 2016)

Most notably, considerable disconnects exist between the severity maps, which are usually produced from passive reflectance based imagery, and forest structural differences that are readily related to changes in aboveground carbon. Often the products developed through the application of spectral indices applied to data is myopically described as "burn severity", a frequently poorly defined term (Keeley, 2009; Lentile et al., 2006). Furthermore, these vaguely defined spectral index-based products are primarily linked to subjective and qualitative observations of likely surface changes (Lentile et al., 2006) that in many cases are inferred without pre-fire data and are often not directly measurable by satellite sensors (Lentile et al., 2009; Roy et al., 2006). Without the development of physical linkages between spectral data and quantitative measures of forest structure, errors in carbon quantification will extrapolate through models, propagating errors (Kolden et al., 2015). A limited number of studies have sought to relate radiometric datasets to mechanistic changes in vegetation following fires (Disney et al., 2011; Smith et al., 2016). Structural datasets such as those derived from LiDAR data have considerable promise to be directly related to changes in vegetation structure (Smith et al., 2014), but such research is limited (Bishop et al., 2014; Wang & Glenn, 2009; Wulder et al., 2009).

Severity delineation from passive sensors is accomplished through the analysis of individual bands (White et al., 1996) or indices that incorporate properties of multiple bands (Lentile et al., 2006; Smith et al., 2007). The most frequently used are the Normalized Burn Ratio (NBR; Lopez-Garcia & Caselles, 1991), delta NBR (dNBR; Key & Benson, 2006), and Relative delta NBR (RdNBR; Miller & Thode, 2007). The dNBR and RdNBR indices are calculated by the Monitoring Trends in Burn Severity (MTBS) project (Eidenshink et al., 2007); these data have subsequently been

used to model pyrogenic emissions (Meigs, Turner, Ritts, Yang, & Law, 2011). The most commonly used field measure of burn severity for calibration of these spectral indices is the Composite Burn Index (CBI) (Key & Benson, 2006), although several limitations to this protocol are apparent. First, because measurements are taken by ocular estimation they can be very subjective (Lentile et al., 2009; Morgan et al., 2014; Zhu et al., 2006). Second, the CBI value is a comprehensive severity score that includes all vertical strata including the subsurface, which correlates poorly to spectral reflectance of the top-most surface (Hudak et al., 2007). Third, because it is a comprehensive score, CBI values are unitless and not directly representative of the ecological metrics that are most relevant to efforts to model and monitor fire effects, such as tree mortality, canopy cover, or carbon consumption. Finally, CBI protocol includes subjective reconstructive estimation of pre-fire conditions in the post-fire environment (i.e., no pre-fire data are usually collected), yielding data of questionable accuracy that are extremely difficult, if not impossible, to verify (Lentile et al., 2006; Morgan et al., 2014; Smith et al., 2016; Zhu et al., 2006).

The difficulty in quantifying fire-induced change without pre-fire measurements extends beyond the CBI protocol. There have been a few rare studies where fire burned through permanent monitoring plots that were subsequently assessed (Bishop et al., 2014; Cocke, Fulé, & Crouse, 2005; Wimberly & Reilly, 2007); however, these studies have relied on small numbers of burned plots to represent change over a large area. Long-term monitoring plots associated with the Forest Inventory and Analysis (FIA) project (Gillespie, 1999) have burned with greater frequency in recent years, but the set return intervals of FIA mean that several years may pass between the fire event and the post-fire re-visit, reducing the visibility and magnitude of those effects when data collection does occur (Whittier & Gray, 2016). The lack of pre-fire observations for the majority of field data utilized to calibrate burn severity spectral indices leads to inconsistency between the remote sensing measures, which quantify change between pre- and post-fire acquisitions, and field calibration measures, which

are limited to post-fire observations. Measuring only the post-fire environment cannot adequately represent the effect of fire, because it fails to capture the magnitude of change, whether the observed changes are in fact directly caused by the fire, or if another disturbance event is also contributing (Roy et al., 2013; Smith et al., 2016; Smith, Eitel, & Hudak, 2010).

The increasing acquisition frequency of airborne Light Detection and Ranging (LiDAR) data over relatively large areas offers a potential alternative mode of measuring fire-induced ecological change and calibrating reflectance-based spectral indices to improve the models that use index-based products. Discrete-return LiDAR collected at high spatial resolution can accurately measure forest height, percent canopy cover, and provide three-dimensional canopy height and density metrics describing the vertical distribution of canopy material, aerodynamic roughness (Hudak et al., 2009; Lefsky et al., 2002), and gap size (Hudak et al., 2009; Kane et al., 2013). Analyzed in concert with field data, LiDAR returns can also be used to predict forest structure attributes such as basal area, volume, biomass, and leaf area (Hudak et al., 2009; Lefsky et al., 2002). LiDAR has been successfully used to quantify the effects of insect outbreaks in forests (Bater et al., 2010; Bright et al., 2012), pre-fire fuel loading (Andersen et al., 2005; Seielstad & Queen, 2003), and structural measurements of the post-fire environment (Bishop et al., 2014; Kane et al., 2013, 2014; Kwak et al., 2010; Wulder et al., 2009). Acquisitions of high-resolution, comparable pre- and post-fire LiDAR data that provide measure of fire-induced vegetation change have been limited (Bishop et al., 2014; Wang & Glenn, 2009; Wulder et al., 2009). However, multi-temporal LiDAR is not a novel concept and has been widely applied to quantify other ecosystem properties such as snow volume (Tinkham et al., 2014), forest growth and harvest disturbance (Hudak et al., 2012), and change in biomass resulting from a Gypsum moth (*Lymantria dispar)* outbreak (Skowronski, Clark, Gallagher, Birdsey, & Hom, 2014), among other applications.

Only two studies to-date have been able to spatially match pre- and post-fire LiDAR acquisitions in order to objectively quantify fire effects on forest structure (Bishop et al., 2014; Wulder et al., 2009), with additional studies by Wang & Glenn (2009) focused on shrubs in steppe ecosystems and Reddy et al. (2015) in peatlands. Neither of the prior studies in forest ecosystems explicitly linked LiDAR-derived forest structure metrics to the spectral indices that are most commonly used to assess forest burn severity across an entire fire; Bishop et al. (2014) assessed the Normalized Differenced Vegetation Index (NDVI) on a small portion of a wildfire, while Wulder et al. (2009) analyzed only a limited set of returns from a single LiDAR transect. In order to model metrics of fire-induced forest change from unitless spectral indices that are widely-utilized to characterize burn severity and model emissions (e.g., dNBR and RdNBR), there is a critical need for additional studies to be undertaken where pre- and post-fire LiDAR overlap spatially.

One such opportunity arose following the 2012 Pole Creek Fire in Central Oregon, USA, where post-fire LiDAR was acquired spatially coincident with a pre-fire acquisition across an entire fire, featuring a gradient of forest types. The primary goal of this study was to assess the accuracy of spectral indices calculated from Landsat imagery in predicting changes in forest structure calculated from pre- and post-fire LiDAR. A secondary objective was to assess the utility of spatial autocorrelation for improving model predictive power. While some studies have sought to improve model predictions of burn severity through inclusion of environmental data at mismatched spatial scales (e.g., Birch et al., 2015; Dillon et al., 2011), simultaneous autoregressive modeling, a form of spatially weighted regression, has been shown to improve on non-spatially explicit regression models (Cressie, 1993; Haining, 1990; Lewis et al., 2011). Simultaneous autoregression incorporates the spatial autocorrelation in burn pattern, providing a proxy for other influential variables (i.e., geomorphic or climatic process) not included in the model (Kissling & Carl, 2007; Prichard &

Kennedy, 2014; Wimberly et al., 2009). These previous findings suggest using a spatially explicit model would improve the relationship between LiDAR metrics and spectral indices.

2. Material and Methods

2.1. Study Area

The study was carried out on the Pole Creek Fire, located along the eastern Cascade Mountains in the Deschutes National Forest, approximately 30 kilometers west north-west of Bend, Oregon (Fig. 1.1). Ignited by lightning on September 9th, 2012, the fire grew to 10,800 hectares before containment in mid-October. The fire burned across a large elevational gradient (1,200 to 2,100 meters) and wide variety of forest types, with dominant tree species including ponderosa pine (*Pinus ponderosa*), lodgepole pine (*Pinus contorta*), mountain hemlock (*Tsuga mertensiana*), and grand/white fir hybrid (*Abies gradis/Concolor*). The mean July minimum and maximum temperatures are 6.3 °C and 23.1 °C, and the mean January minimum and maximum temperatures are -6.0 °C and 2.1 °C. In an average year, the area receives 1095 millimeters of precipitation, mostly as snow (PRISM Climate Group, Oregon State University, http://prism.oregonstate.edu, created 6 September 2015). Mountain pine beetle (*Dendroctonus ponderosae*) caused significant mortality throughout the *P. contorta* stands 6-12 years before the fire (McCarley, Kolden, Vaillant, Hudak, and Smith, *Chapter 2*, this thesis).

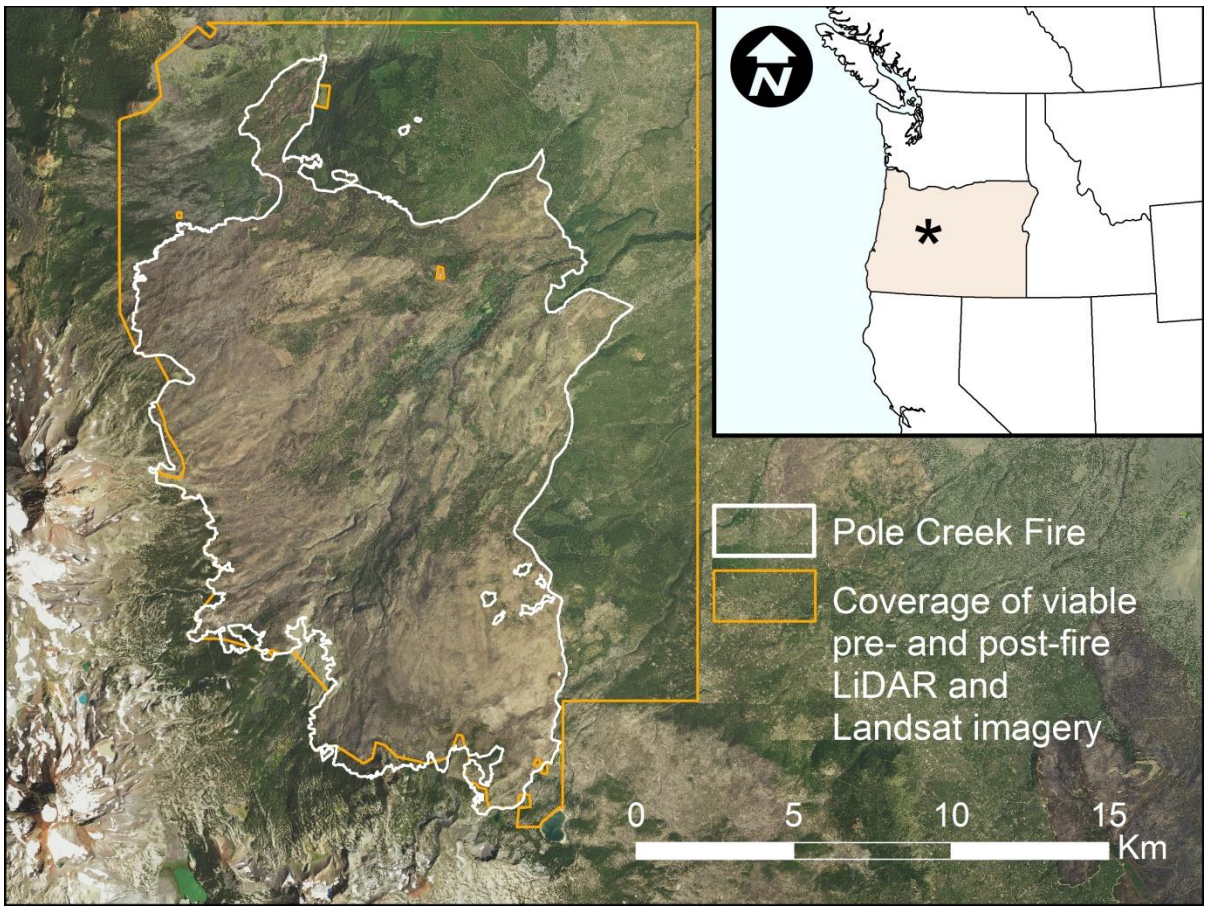

Figure 1.1: Location of Pole Creek Fire (white outline) in central Oregon and the overlap of viable LiDAR and Landsat imagery (orange outline with crosshatch). Data overlaid on 2014 National Agricultural Imagery Program (NAIP) imagery.

2.2. Data Pre-processing

Pre- and post-fire USGS Level 1 terrain-corrected (L1T) Landsat TM and OLI scenes were selected (Table 1.1) on the basis of phenological comparability, nonexistence of snow or cloud cover over the burn area, and maximizing the number of pixels for analysis. Based on the criteria all pre-fire scenes from 2012 were excluded because the scan line error on Landsat ETM+ reduced the number of useable pixels considerably. Remaining candidate scenes were evaluated for best match based on plant phenology and sun angle following best practices of Key (2006). All of the scene combinations had a few patches of snow at higher elevations, creating interference with change analysis. Therefore,

pixels containing snow were excluded once the best phenological pair was determined. For similar reasons open water bodies with seasonally variable levels were also excluded, resulting in the omission of 1.6% of the pixels within the fire perimeter. In order to prepare and standardize Landsat scenes for multi-date comparison, band brightness values were transformed into reflectance (Chander & Markham, 2003), then atmospherically corrected to at-surface-reflectance using the Cos(t) model and Dark Object Subtraction (Chavez, 1996).

Discrete, multi-return LiDAR data were acquired pre- and post-fire by Watershed Sciences, Inc. (Corvallis, OR) (Table 1.1) at a survey altitude of 900 meters above ground level with a 28° field of view (± 14° from nadir) and at least 50% side-lap. In each case, the vendor post-processed the LiDAR data in order to ensure geometric accuracy and develop a 1-meter digital terrain model. Following delivery, pre- and post-fire data were height normalized by subtracting the terrain model from the LiDAR point cloud using the USDA Forest Service's FUSION software package (http://forsys.cfr.washington.edu/fusion.html). Pre-fire LiDAR data were re-projected using LAStools (Isenburg, 2013) from state plane into UTM to match the post-fire LiDAR and Landsat data.

Table 1.1: Data Acquisition Parameters

	Date	Sensor Type	Resolution
Pre- Fire LiDAR	October 7-11, 2009	Leica ALS50	Average 8 pulses/m^2
Pre- Fire Multi-spectral Image[a]	July 23, 2011	Landsat 5 TM[b]	Bands 1-5 and 7, 30-m Band 6 (thermal), 120-m
Post- Fire Multi-spectral Image[a]	June 10, 2013	Landsat 8 OLI[b]	Bands 1-7 and 9, 30-m Bands 10 and 11 (thermal), 100-m Band 8 (panchromatic), 15-m
Post-Fire LiDAR	October 8-11, 2013	Leica ALS50	Average 8 pulses/m^2

[a] Scene located at Worldwide Reference System 2: Path 45, Row 29. [b] Despite the differences in spectral channel and bit size between Landsat 8 and the two previous missions (Landsat 5 and 7), there is no discernable difference in spectral signature of burned surfaces (Koutsias & Pleniou, 2015).

2.3. Spectral Indices

Fifteen spectral indices were selected based on their use in other studies that mapped fire effects. These, as well as individual Landsat bands converted to at-surface reflectance were used as predictor variables for LiDAR-derived structure metrics in the analysis. Indices were calculated per equations provided in seminal papers (Table 1.2). Following practices by Key (2006) and Cansler & McKenzie (2012), an offset value was applied that accounted for phenological differences between the pre- post-fire images. This required identifying a few homogenous-forested areas outside the fire perimeter for reference and computing the mean value for each spectral index in those areas. Understanding that the reference areas should have a differenced index value of zero, adjustments were made to all the pixel values by adding or subtracting the value of the reference mean.

Table 1.2: Remotely Sensed Spectral Predictors

Change Spectral Index	Derivation	Key Reference
Δ Landsat Bands (Blue **(dB)**, Green **(dG)**, Red **(dR)**, Near Infrared **(dNIR)**, Shortwave Infrared 1 **(dSWIR1)**, and Shortwave Infrared 2 **(dSWIR2)**)	-	-
Δ Normalized Burn Ratio **(dNBR)**	$(\rho_{NIR}-\rho_{SWIR2}) / (\rho_{NIR}+\rho_{SWIR2})$	(Key & Benson, 2006)
Relative dNBR **(RdNBR)**	$dNBR / \sqrt{(\lvert NBR_{pre}\rvert)}/1000$	(Miller & Thode, 2007)
Δ Normalized Differenced Vegetation Index **(dNDVI)**	$(\rho_{NIR}-\rho_{r}) / (\rho_{NIR}+\rho_{r})$	(Rouse, Haas, Deerling, Schell, & Harlan, 1974)
Δ Mid-Infrared Bi-Spectral Index **(dMIRBI)**	$10\rho_{SWIR2}-9.8\rho_{SWIR1}+2.0$	(Trigg & Flasse, 2001)
Δ Char Soil Index **(dCSI)**	$\rho_{NIR} / \rho_{SWIR1}$	(Smith et al., 2007)
Δ Soil Adjusted Vegetation Index **(dSAVI)**	$(\rho_{NIR}-\rho_{r})(1+L) / (\rho_{SWIR1})$	(Huete, 1988)
Δ Tasseled Cap Brightness **(dTCB)**, Greenness **(dTCG)**, and Wetness **(dTCW)**	$(\rho_{b}*\varepsilon) + (\rho_{g}*\varepsilon) + (\rho_{r}*\varepsilon) + (\rho_{NIR}*\varepsilon) + (\rho_{SWIR1}*\varepsilon) + (\rho_{SWIR2}*\varepsilon)$	(Crist, 1985; Kauth & Thomas, 1976)
Δ The first three Principle Components **(dPC1, dPC2, dPC3)**	$(dB*\alpha) + (dG*\alpha) + (dR*\alpha) + (dNIR*\alpha) + (dSWIR1*\alpha) + (dSWIR2*\alpha)$	(Patterson & Yool, 1998)
Δ Normalized Differenced Water Index **(dNDWI)**	$(\rho_{NIR}-\rho_{SWIR1}) / (\rho_{NIR}+\rho_{SWIR1})$	(Gao, 1996)
Δ Band 7/4 Ratio **(d74)**	$\rho_{SWIR2} / \rho_{NIR}$	(Kushla & Ripple, 1998)
Δ Band 7/5 Ratio **(d75)**	$\rho_{SWIR2} / \rho_{SWIR1}$	(Epting, Verbyla, & Sorbel, 2005)

All Spectral Indices analyzed as the difference from pre- to post-fire; ρ = at-surface reflectance for band ρ_x, where x is given by the Landsat sensor. L=soil constant set to 0.5. ε = coefficients for linear transformation, defined by Crist (1985). α = coefficients for principle component analysis were derived from pixels within the fire using an unstandardized principle component transform (based on covariance matrix) and are defined in the appendix.

2.4. LiDAR Metrics

The metrics used in this study (Table 1.3) were selected based on use in other forestry applications (e.g., Hudak et al., 2012; Wing et al., 2012), comparability with fire-effects strata assessed in CBI (Key & Benson, 2006), and theoretical sensitivity to fire effects. Based on the recommended definition of surface fuel by Brown, Oberhau, & Johnston (1982), this study used a 1.8 meter threshold for calculating canopy cover (above 1.8 meters) and mean surface fuel height (below 1.8 meters).

The LiDAR point cloud was binned to a 30-meter grid, designed to match the layout of the Landsat pixels, and produced a series of descriptive statistics for each cell using the GridMetrics tool in FUSION. Selected statistics were then converted to a raster grid using the CSV2Grid function and the raster calculator in ArcGIS was used to compute the differenced metric. In all cases, both an absolute change (pre – post) and a relative change ((pre – post) / pre) value was calculated.

Table 1.3: LiDAR Metrics of Forest Structure

LiDAR Metric	Interpretation
pre – post	
Mean of returns ≥ 0.15 m	Δ Mean vegetation height **(dMHT)**
Standard deviation of returns ≥ 0.15 m	Δ Vegetation height standard deviation **(dSD)**
Skewness value of returns ≥ 0.15 m	Δ Vegetation height skewness **(dSKW)**
Percent of returns < 1 m	Δ Percent returns herbs, low shrubs, and debris < 1 m **(dS1)**
Percent of returns ≥ 1 m and ≤ 5 m	Δ Percent returns tall shrubs and trees 1 – 5 m **(dS2)**
Percent of returns > 5 m and ≤ 8 m	Δ Percent returns tall shrubs / intermediate trees **(dS3)**
Percent of returns > 8 m and ≤ 20 m	Δ Percent returns intermediate trees / upper canopy **(dS4)**
Percent of returns > 20 m	Δ Percent returns upper canopy **(dS5)**
Mean height of returns ≤ 1.8 m	Δ Mean surface fuel height **(dMSFH)**
Percent of returns > 1.8 m	Δ Percent Canopy Cover **(dCC)**
Using vegetation heights: (mean – min) / (max – min)	Δ Canopy Relief Ratio **(dCRR)**
Mean vegetation height * canopy cover	Δ Canopy Density **(dCD)**
(pre - post) / pre	
Mean of returns ≥ 0.15 m	Relative Δ Mean vegetation height **(RdMHT)**
Standard deviation of returns ≥ 0.15 m	Relative Δ Vegetation height standard deviation **(RdSD)**
Skewness value of returns ≥ 0.15 m	Relative Δ Vegetation height skewness **(RdSKW)**
Percent of returns < 1 m	Relative Δ Percent returns herbs, low shrubs, and debris < 1 m **(RdS1)**
Percent of returns ≥ 1 m and ≤ 5 m	Relative Δ Percent returns tall shrubs and trees 1 – 5 m **(RdS2)**
Percent of returns > 5 m and ≤ 8 m	Relative Δ Percent returns tall shrubs / intermediate trees **(RdS3)**
Percent of returns > 8 m and ≤ 20 m	Relative Δ Percent returns intermediate trees / upper canopy **(RdS4)**
Percent of returns > 20 m	Relative Δ Percent returns upper canopy **(RdS5)**
Mean height of returns ≤ 1.8 m	Relative Δ Mean surface fuel height **(RdMSFH)**
Percent of returns > 1.8 m	Relative Δ Percent Canopy Cover **(RdCC)**
Using vegetation heights: (mean – min) / (max – min)	Relative Δ Canopy Relief Ratio **(RdCRR)**
Mean vegetation height * canopy cover	Relative Δ Canopy Density **(RdCD)**

2.5. Model Comparison

Due to the high number of insignificant models, a preliminary screening was conducted of all combination pairs of spectral indices and LiDAR metrics using a Pearson's correlation. Poorly correlated pairs (less than an absolute value of 0.5) were eliminated from further evaluation. The remaining pairs were assessed using pairwise ordinary least squares (OLS) regressions and comparing their r-squared values.

All statistics was computed in the software R (R Development Core Team, 2014) and applied the simultaneous autoregressive model using the 'spdep' package (Bivand, 2002), following the equation:

$$Y = X\beta + \lambda W(Y - X\beta) + \varepsilon$$

where Y is the dependent variable, X is the explanatory variable, β is the vector of coefficients, λ is the autoregressive coefficient, W is the row-standardized matrix of spatial weights, and ε is the uncorrelated error term (Cressie, 1993; Haining, 1990). The spatial weights matrix was defined to give weight to pixels within a pre-defined neighborhood based on the inverse of the distance from focal center to the center of neighboring pixels. These values were then row-standardized, giving the neighboring pixels a total summed weight of one, and all other pixels a weight of zero. Following the recommendation of Kissling & Carl (2008) and practice of other wildfire studies incorporating simultaneous autoregression (Meigs et al., 2016; Prichard & Kennedy, 2014), neighborhood pixels were defined as those centered within 60 meters because that distance minimized Akaike's Information Criterion (AIC; Akaike, 1974) and residual spatial autocorrelation over other possible neighborhood distances. Due to the large number of observations, this study used a Chebyshev sparse matrix approach that estimates the autoregressive coefficient rather than calculating it directly from eigenvalues (Pace & LeSage, 2004). This method allowed application of the model to a much larger

area than would be computationally possible otherwise, avoiding having to subsample the data as others have (Lewis et al., 2011; Wimberly et al., 2009).

The outputs of each model pair were compared in order to test the hypothesis that the spatially explicit model would provide a superior model to OLS. Using R, the simultaneous autoregression produces a Nagelkerke pseudo-r-squared (Nagelkerke, 1991), which is not directly comparable to an OLS r-squared. Therefore AIC was used to show improvement; however, the pseudo-r-squared value was an acceptable method to compare correlations between spectral indices and LiDAR metrics.

3. Results

R-squared values for the 63 viable OLS regression models were plotted in a matrix to examine the magnitude and quality of the relationships between spectral indices and LiDAR metrics (Fig. 1.2). The best-observed relationship was between d74 and dCC ($r^2 = 0.63$), followed by d75 and dCC ($r^2 = 0.62$), dSWIR2 and dCC ($r^2 = 0.52$), and dMIRBI and RdCC ($r^2 = 0.52$). For dSWIR2, dNBR, dNDVI, dTCW, dPC1, d74 and d75, the highest r-squared values corresponded to dCC. For dB, dG, dSAVI, and dNDWI, dCC was the only LiDAR metric that passed preliminary screening. The worst r-squared value for a model not eliminated was between dPC1 and RdS2 ($r^2 = 0.25$). All models were statistically significant, even poorly performing ones due to the extremely large sample size (n = 117,520).

This study compared AIC values for the spatially explicit and OLS models for each of the 63 viable pairs (Fig. 1.3). For all pairs the AIC value was lower using simultaneous autoregression, indicate model improvement. The biggest decrease in AIC was observed for dSAVI and dCC, while the smallest was between d75 and RdS2. Across spectral indices dCC and dS4 saw the greatest benefit from simultaneous autoregression. RdS2 was the least improved LiDAR metric for all spectral

indices. Pseudo-r-square values were also generated and plotted for each of the model pairs (Fig. 1.4). With spatial autocorrelation accounting for the influence of unknown predictor variables, the best-observed relationship was still d74 and dCC (psedo-r^2 = 0.86), followed by dNBR and dCC (psedo-r^2 = 0.85), dNDVI and dCC (psedo-r^2 = 0.84). dSWIR2 and dCC (psedo-r^2 = 0.84), dPC1 and dCC (psedo-r^2 = 0.84), dNDWI and dCC (psedo-r^2 = 0.84), and dTCG and dCC (psedo-r^2 = 0.84) were all close behind. dCC was the best predicted LiDAR metrics for all spectral indices (psedo-r^2 ranging from 0.79 to 0.86), followed by dS4, RdCC, and dS3. RdS2 uniformly had the weakest correlations to all spectral indices (psedo-r^2 ranging from 0.45 to 0.47).

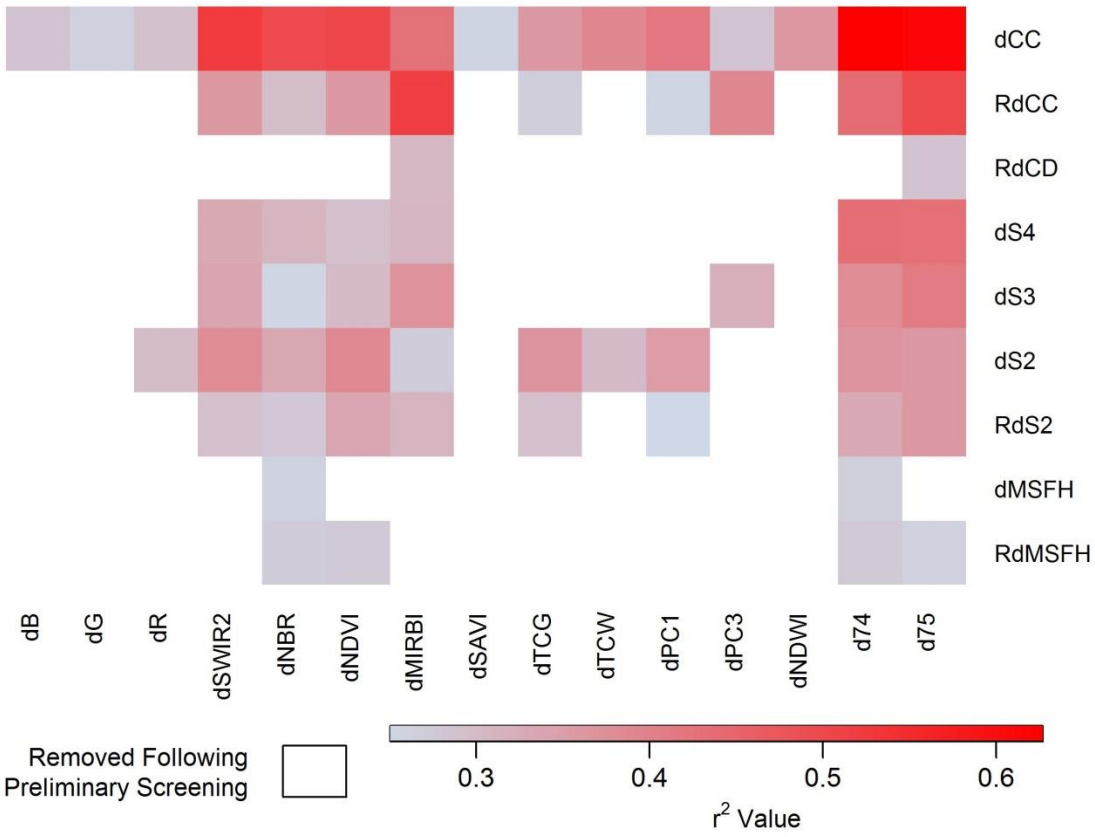

Figure 1.2: Comparison of R-Squared values for pairwise ordinary least squares (OLS) regression between LiDAR metrics and spectral indices. Models with a Pearson's Correlation below an absolute value of 0.5 omitted (preliminary screening). Acronyms defined in Table 1.2 and 1.3.

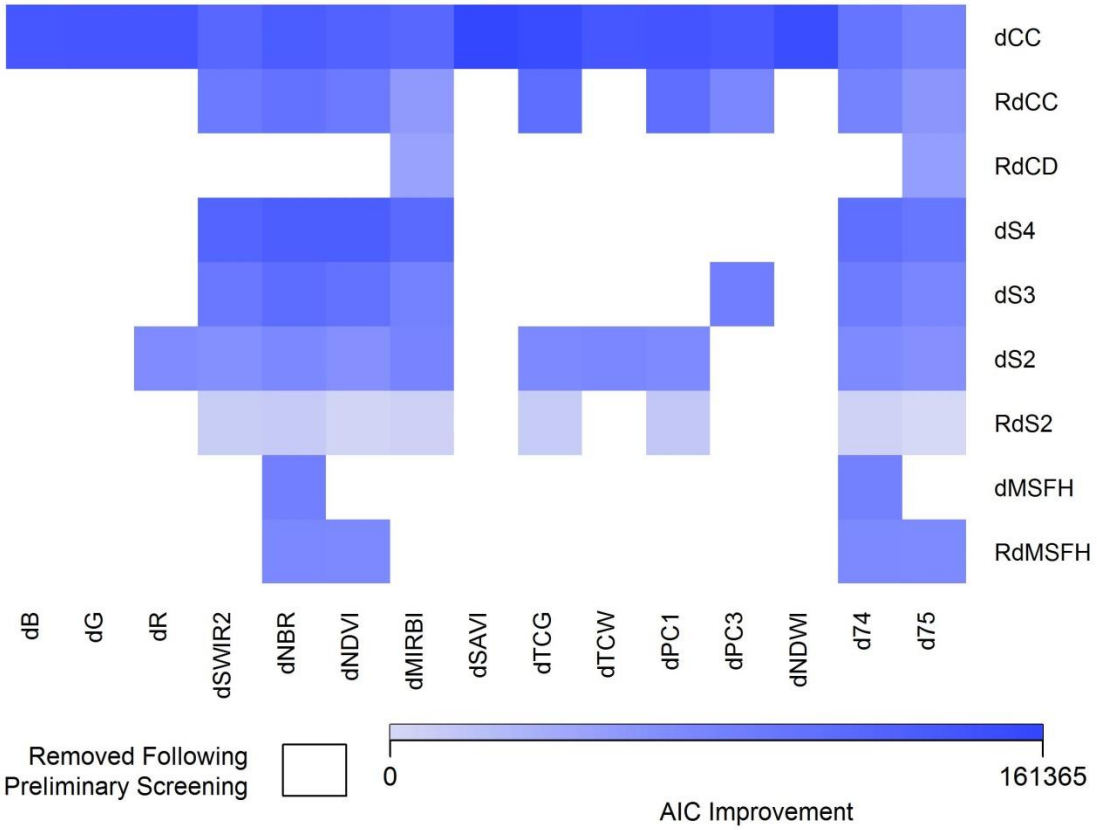

Figure 1.3: Improvement over ordinary least squares (OLS) models through the use of simultaneous autoregressive (SAR) modelling measured by Akaike information criterion (AIC) values (positive indicates improvement, zero no change, and negative suggests worsening). Models with a Pearson's Correlation below an absolute value of 0.5 omitted (preliminary screening). Acronyms defined in Table 1.2 and 1.3.

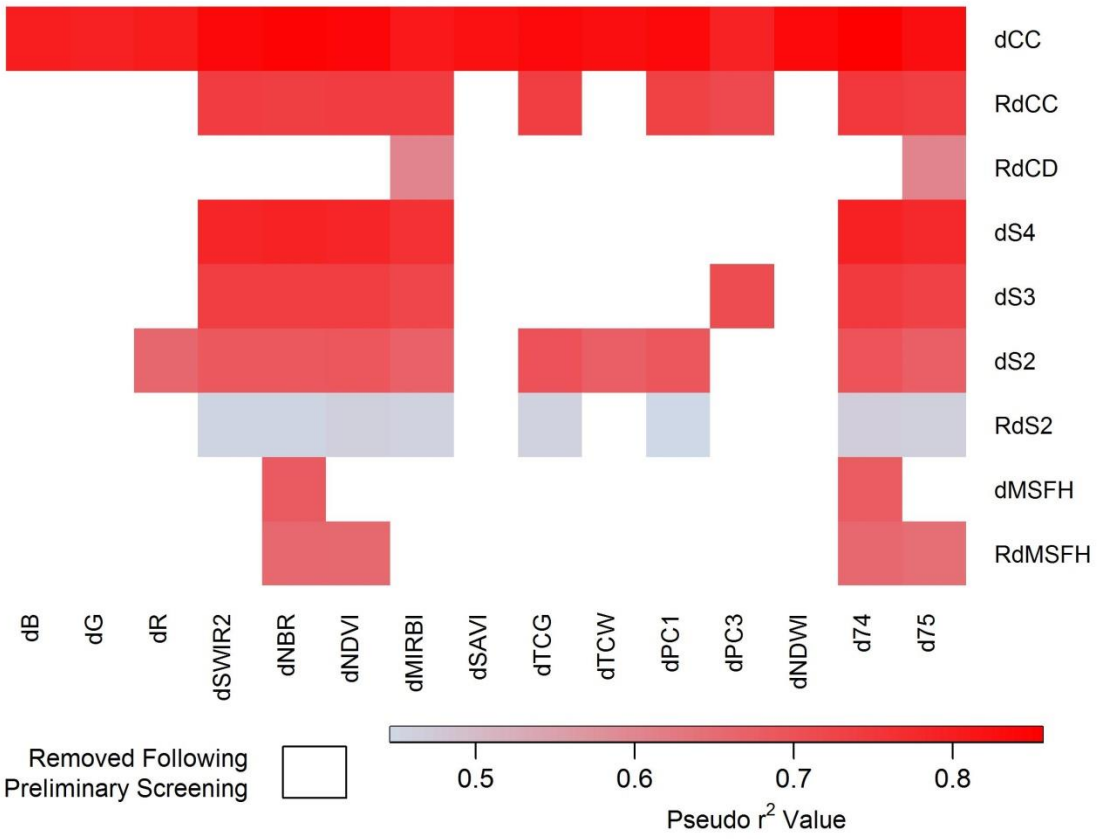

Figure 1.4: Comparison of pseudo-r-squared values for simultaneous autoregressive (SAR) modelling between LiDAR metrics and spectral indices; models with a Pearson's Correlation below an absolute value of 0.5 omitted (preliminary screening). Acronyms defined in Table 1.2 and 1.3.

4. Discussion

4.1. Canopy Cover

The results suggest that LiDAR estimated change in canopy cover is the primary biophysical fire effect detected by spectral remote sensing, since that metric produced the best correlation with all spectral indices. The finding that changes in the top-most-surface is more detectable by spectral remote sensing than any other structural change is supported by other studies. Using fires across the western U.S., Hudak et al. (2007) demonstrated that primarily the surface cover fractions rather than

understory vegetation or soil effects influenced spectral response. Field estimates of change in canopy cover using the Forest Vegetation Simulator (FVS; Dixon, 2002) also have an established relationship with RdNBR in California ecosystem (Miller & Quayle, 2015; Miller, Knapp, et al., 2009). Absolute change in canopy cover derived from a LiDAR line transect was also the best correlated metric to post-fire NBR, dNBR, and RdNBR using all data points in a boreal forest ecosystem (Wulder et al., 2009).

Using simultaneous autoregression, the indices that had the best relationship to dCC were d74 and dNBR, both of which use the SWIR2 and NIR bands. The individual SWIR2 band had a strong relationship with dCC, while dNIR was a strong predictor only when used in combination with other bands (i.e., d74, dNBR, dNDVI). Many other studies have indicated that SWIR2 and NIR provide the best correlation with field measurements incorporating fire effects on all strata (Key & Benson, 2006; Miller & Yool, 2002; van Wagtendonk et al., 2004; White et al., 1996). Based on these findings, SWIR2 appears to be the most sensitive band for detecting fire-induced changes for canopy cover.

4.2. LiDAR Metrics

The change in percent of returns below 1 meter (dS1) appeared to be influenced primarily by topography, either because of fire behavior in this stratum or as an artifact from height normalization of the LiDAR data. In either case, dS1 or RdS1 were not well correlated with spectral indices. Mean surface fuel heights (dMSFH and RdMSFH) were also not well correlated, but did reveal a distinct trend. At low levels of spectral change, dMSFH and RdMSFH varied considerably, but at higher levels of spectral change they exhibited decreasing fuel heights consistent with expected consumption. The low correlation and extreme variation at low severity levels might suggest that spectral remote sensing is not fully able to detect changes in the understory when canopy is intact.

Moving up the strata to change in percent returns 1-5 meters (dS2) and up through percent of returns from 5-8 meters (dS3) and percent of returns from 8-20 meters (dS4), correlations with spectra gradually improved. Other than changes in canopy cover (dCC and RdCC), the best correlated LiDAR metrics were dS3 and dS4. The model improvements observed with increasing height strata highlight the difficulty of measuring reflectance values anywhere but the top-most-surface. The exception to this trend was the poor correlation observed between change in percent returns above 20 meters (dS5) and the spectral indices. While 73% of pixels had pre- and post-fire LiDAR returns above 20 meters, they were usually few in number, having a median value of only 3-4% of all returns in the pixels having returns in that strata. Therefore, the poor correlation between dS5 or RdS5 and any of the spectral indices might be a result of the dearth of vegetation in most areas at those strata (largely treetops) and the consequential influence from spectral reflectance in the stratum below.

Models using relative delta LiDAR metrics also had lower pseudo-r-squared values than their absolute delta counterparts did, indicating that for this type of forested ecosystem absolute measures of change were easier to detect using spectral remote sensing. In a similar study, Wulder et al. (2009) tested post-fire NBR, dNBR, and RdNBR against absolute and relative change in structure derived from a LiDAR transect. Their work does not indicate significant differences in model quality between absolute and relative change, but their sample size was considerably smaller (n = 67) than ours and in a notably different ecosystem. All of the relative delta LiDAR metrics tested also tended to emphasize change opposite from fire effects due to outliers experiencing extremely negative values. The relative delta metrics could not exceed a value of one, which represents complete change from pre-fire condition. However, there was no theoretical limit in the opposite direction, so in places where post-fire values were much higher than pre-fire values, wildly negative values resulted.

Classic statistical metrics derived from the LiDAR point cloud (i.e., mean height, standard deviation, and skewness) did not perform well and were removed during preliminary screening.

RdCD, which is a function of mean height and canopy cover, was included in the analysis and modelled with dMIRBI and d75. However, the pseudo-r-squared values were among the lowest for the spatially explicit model, indicating little evidence of a relationship between classic statistical measurements of the point cloud and spectral change.

4.3. dNBR and RdNBR

Because of their widespread use and adoption into MTBS, a discussion of dNBR and RdNBR is warranted. In this study, dNBR outperformed RdNBR across all structural metrics. This was foremost the result of two distinctly different relationships observed between RdNBR and the LiDAR metrics (Fig. 1.5). Further investigation revealed that in areas where pre-fire NBR was near zero and post-fire NBR was negative, the RdNBR equation produced unreasonably high values that do not fit into a linear or non-linear model. McCarley et al. (*Chapter 2*, this thesis) determined that these areas corresponded to where pre-fire mountain pine beetle mortality had occurred. These results not only contradict studies that suggest RdNBR would perform better in forests where pre-fire disturbance has resulted in heterogeneous vegetation cover (Miller & Thode, 2007), but also raise questions regarding recent studies that have assessed the impact of mountain pine beetle outbreaks on subsequent fire severity utilizing RdNBR as a proxy for burn severity (Meigs et al., 2016; Prichard & Kennedy, 2014).

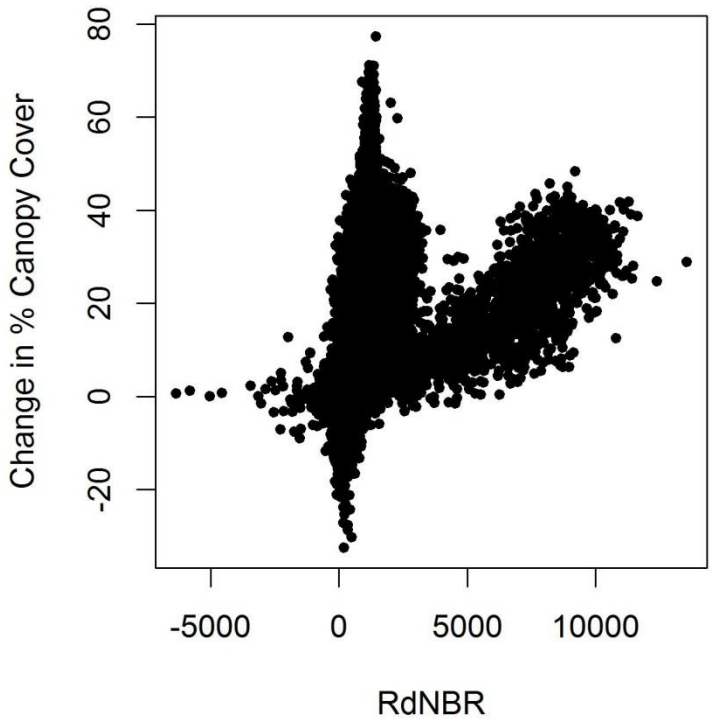

Figure 1.5: Scatterplot of the Relative delta Normalized Burn Ratio (RdNBR) and change in percent canopy cover measured by LiDAR**.**

For this fire, dNBR was slightly outperformed in the prediction of all of the LiDAR metrics except dMSFH and RdMSFH by d74, a simple ratio utilizing the same Landsat bands as dNBR. Nonetheless, significant evidence was not observed indicating d74 would make a clearly superior index. Furthermore, the use of the normalized form may produce results that are more consistent when comparing fires across regions and with differing levels of scene illumination (Key & Benson, 2006). dNDVI and dNBR performed similarly when compared with dCC, and mirrored each other in comparison with the other LiDAR metrics. Hudak et al. (2007) also reported similarities in performance between post-fire NDVI and NBR when predicting field measures of fire effects, although their study indicated weaker (although not significantly) values of dNDVI. These results

suggest that dNDVI may be useful when Shortwave Infrared (SWIR) data are not available, but the strong correlations found with SWIR2 suggest that dNBR is a better burn severity index.

4.4. Spectral Indices

SWIR2 was the individual band with the best relationship to structural change. dCC was weakly correlated to dB, dG, and dR. A better relationship with dNIR or dR and dCC was expected given the sensitivity of these bands to fire-induced changes in vegetation (Chuvieco, Martín, & Palacios, 2002; Rogan & Yool, 2001). However, the poor relationship with dNIR is consistent with Smith et al. (2009), who demonstrated that near infrared reflectance was insensitive to mean LiDAR plot height. Although a strong correlation was not observed between dNIR or dR, dNDVI was a good indicator of LiDAR metrics, particularly change in canopy cover.

While all of the spectral indices tested produced better correlations with dCC than RdCC, d74 was most suited to predicating relative measures of change. One limitation to this conclusion is that no relative spectral indices were used other than RdNBR (which was eliminated from analysis due to the extreme values produced in some areas, as noted above). While the use of other relative indices may provide better relationships to relative LiDAR metrics, evidence was not observed suggesting that they would outperform the relationships observed by this study.

4.5. Simultaneous Autoregressive Model

All models were improved by the use of simultaneous autoregression, supporting its value for landscape assessment of fire effects (Meigs et al., 2016; Prichard & Kennedy, 2014; Wimberly et al., 2009). The greatest improvement in AIC was for dCC, which was already the best-predicted structural change measure. Prior attempts to model burn severity across landscapes and understand drivers of burn severity have found topography to be the strongest predictor of burn severity (Birch et

al., 2015; Dillon et al., 2011). However, these studies note the limitations of trying to predict burn severity at 30-meter spatial resolution utilizing predictor variables such as climate and weather, which are only available at coarser spatial resolutions. This suggests that spectral indices using a simultaneous autoregressive model might be the best proxy for specific biophysical measures of change (i.e., change in canopy cover), as it allows for consideration of additional explanatory environmental variables known to contribute to fire behavior such as climate, topography, and vegetation, without requiring that these variables be included in the models (Kissling & Carl, 2007).

4.6. Future Work

One obvious limitation is that this study was conducted on a single fire, thus the potential for these models to be applied regionally or globally is uncertain. Nonetheless, the primary objective was not to establish a universal model between spectral remote sensing and structural change, but to validate the utility of Landsat spectral change indices by exploiting the opportunity afforded by the availability of pre- and post-fire LiDAR collections. LiDAR provides a physical measure of vegetation structure change that can be binned at a resolution to commensurate with Landsat. The correlations observed suggest that further study is warranted in other vegetation types, but as acquisition of LiDAR data increases, more pre- and post-fire datasets will be available to replicate this validation of Landsat sensor-derived spectral indices of burn severity. The need to define ecosystem-specific models that predict specific fire-induced forest structural change metrics at regionally significant scales is documented (Kolden et al., 2015), but as long as LiDAR remains cost-prohibitive, a robust spectral proxy derived from freely available Landsat data can provide effective measures of biophysical change that managers and scientists need.

In this study, all LiDAR points were analyzed regardless of other attributes. However, recently other studies have introduced the possibility of separating live and dead LiDAR returns using

intensity values (Kim et al., 2009; Wing, Ritchie, Boston, Cohen, & Olsen, 2015). This analysis may enhance future models since change in live canopy cover would likely be better correlated to spectral change.

LiDAR also offers the opportunity to derive useful data such as biomass, basal area, or leaf area index in places where field calibration sites are available (Hudak et al., 2009; Lefsky et al., 2002). The relationship between spectral data and these measurements may offer insights that structural metrics cannot. Given the importance of accurately modelling carbon emissions, LiDAR derived measures of change in biomass may prove critical in continuing to evaluate the ability for spectral remote sensing to measure emissions and be scalable regionally and globally.

Finally, the issues observed with RdNBR in areas experiencing pre-fire mountain pine beetle mortality suggest a need to explore the effect of pre-fire disturbance on the ability to accurately model fire effects across a mosaic of forest histories. While numerous studies have examined the relationship between mountain pine beetle and burn severity (e.g., Agne et al., 2016; Harvey, Donato, & Turner, 2014; Meigs et al., 2016), none have addressed this issue at the landscape scale using measures of severity other than reflectance. The availability of pre- and post-fire LiDAR presents a rare opportunity to understand the effect of mountain pine beetle on subsequent structural change cause by wildfire.

5. Conclusions

This work helps address a critical gap in understanding the relationship between biophysical fire effects and spectral remote sensing by using multi-temporal LiDAR across an entire fire to measure fire-induced structure change. The use of LiDAR bypasses the primary difficulty with comparing multi-temporal spectral data to field measurements, which is the lack of pre-fire field observations. In this analysis, certain spectral indices, most notably dNBR, successfully detected

change in canopy cover. Accurate detection of structural change in lower forest strata were not observed, suggesting that spectral remote sensing is primarily limited to detecting fire-induced changes in the top-most-surface. This finding is significant given the current use of reflectance data to evaluate post-fire habitat, secondary fire effects (i.e., flooding and erosion), comprehensive severity ratings, and carbon emissions. As LiDAR coverage increases spatially and temporally, there will be opportunities to validate reflectance-based spectral indices to structural measures of change derived from LiDAR with high confidence at a commensurate scale.

Chapter 2: Landscape-scale Quantification of Fire Effects Following Mountain Pine Beetle Epidemic and Timber Harvest

T. Ryan McCarley, Crystal A. Kolden, Nicole M. Vaillant, Andrew T. Hudak, Alistair M.S. Smith

In preparation for *Forest Ecology and Management*

Abstract

Across the western United States, bark beetles, timber harvest, and wildfire are three primary drivers of tree mortality and carbon balance. While these agents of forest change frequently overlap spatially, uncertainty remains regarding their interactions and impacts, particularly the influence of insect outbreaks on subsequent fire effects. Acquisition of pre- and post-fire Light Detection and Ranging (LiDAR) data on the 2012 Pole Creek Fire in central Oregon provided a unique opportunity to isolate quantitative fire effects from other agents of change across an entire wildfire. This study characterizes the influence of pre-fire MPB and harvest disturbances on LiDAR-estimated change in canopy cover. Consistent with the literature, a lower reduction of estimated canopy cover was observed for areas where timber harvest occurred pre-fire. However, in contrast to several recent studies in the same region, a greater loss of forest canopy was observed in areas experiencing pre-fire MPB. Notably, this trend was observed even when accounting for heterogeneity in pre-fire canopy cover. Harvest treatment type was not as important as time since treatment, and consistent with the literature, the estimated reduction in canopy cover was observed to be greater in older stands. However, these results suggest that further research is critically needed to understand the complexity of MPB, timber harvest, and wildfire interactions.

Keywords: wildfire, LiDAR, canopy cover, eastern Cascades, fuel treatments

1. Introduction

Climate change is facilitating large-scale ecological disturbance, including potential increases in larger, more intense wildfires (Barbero et al., 2015; Littell et al., 2009; Westerling et al., 2006) and bark beetle outbreaks that have reached levels unprecedented for the previous 125 years (Raffa et al., 2008). When considered along with timber harvest, these agents of forest change represent three of the most significant drivers of tree mortality across the western United States (Hicke, Meddens, & Kolden, 2015). Bark beetle epidemics preceding wildfire have been hypothesized to impact both wildfire severity and carbon emissions through alteration of pre-fire fuel loading (Hicke et al., 2012; Hicke, Meddens, Allen, & Kolden, 2013; Meigs et al., 2009). Timber management activities, including fuel treatments, have been shown to strongly influence subsequent wildfire effects, primarily by reducing fire intensity (Moghaddas & Craggs, 2007; Pollet & Omi, 2002; Prichard et al., 2010; Safford et al., 2009, 2012). The intersection of these events is inevitable, so understanding the consequences and uncertainties of their combined impacts is critically relevant to forest managers. While there has been extensive efforts made to understand how individual agents acting over relatively small portions of a fire have influenced subsequent fire effects, there is a considerable knowledge gap concerning how agents of change interact over longer temporal periods and across larger areas.

Fire effects are commonly referred to as “fire” or “burn” severity, which although sometimes used interchangeably, are usually defined by the temporal scale of analysis, with fire severity referring only to immediate effects (Lentile et al., 2006). Both these terms are notoriously ambiguous, having been used to describe a range of specific vegetation and soil effects or used more broadly without linkage to quantitative physical processes (Keeley, 2009; Lentile et al., 2006). Severity is frequently measured at the landscape scale using spectral indices derived from passive spaceborne

remote sensing platforms (Lentile et al., 2006). The delta Normalized Burn Ratio (dNBR; Key and Benson, 2006; Lopez-Garcia and Caselles, 1991) and the Relative dNBR (RdNBR; Miller and Thode, 2007) are the most widely used spectral indices in the USA, primarily because dNBR and RdNBR raster products are distributed by the Monitoring Trends in Burn Severity (MTBS) project for all U.S. fires greater than 202 hectares in the east, and 404 hectares in the west (Eidenshink et al., 2007). Empirical relationships between these products and fire effects on the ground are established using specific biometric fire effects (e.g., Hudak et al., 2007; Miller and Quayle, 2015) or comprehensive, albeit highly subjective sampling protocols such as the Composite Burn Index (CBI; Key and Benson, 2006) or Geometrically Structured CBI (GeoCBI; De Santis & Chuvieco, 2009). However, CBI has not performed well across all ecosystems (Kasischke et al., 2008) and so dNBR and RdNBR, which were originally developed through empirical correlation with CBI, are often applied without field validation (Baker, 2015; Meigs et al., 2016), introducing significant uncertainty into what biological component or functionality is actually being measured (Kolden et al., 2015). Even when spectral indices are correlated to quantitative field measurements, the vast majority of studies lack pre-fire observations and instead rely upon estimation of the pre-fire conditions, thus failing to objectively capture the true magnitude of change (Roy et al., 2013; Smith et al., 2016, 2010). It is also difficult to address landscape fire effects using field measurements alone, as many wildfires are in remote areas with difficult terrain and few access roads. This limits field samples to parts of the fire that are safely accessible (Cansler & McKenzie, 2012; Hoy, French, Turetsky, Trigg, & Kasischke, 2008; Hudak et al., 2007; Key & Benson, 2006), making it very difficult to control for only the agents of change in an experimental framework and potentially causing a source of bias. Furthermore, while such studies may be able to capture the variability of post-fire effects as indicated from the spectral data (e.g., Landsat) in the accessible sampled area, the observed variation in the spectral index may not be the best judge of the true surface variability.

Although recent studies have explored the effects of antecedent bark beetle outbreaks on burn severity, there remain significant limitations in understanding this interaction. Most have only analyzed a limited number of ground-based observations and have not demonstrated the scaling up of these observations and/or their relationship to remotely-sensed indices (Agne et al., 2016; Harvey et al., 2014a, 2014b; Schoennagel, Veblen, Negron, & Smith, 2012; Simard, Romme, Griffin, & Turner, 2011). Studies analyzing spectral data across landscapes have lacked empirical relationships between spectral reflectance and specific biometric fire effects (Bigler, Kulakowski, & Veblen, 2005; Kulakowski & Veblen, 2007; Meigs et al., 2016), or validated reflectance using only CBI (Bond, Lee, Bradley, & Hanson, 2009; Prichard & Kennedy, 2014). Table 2.1 synthesizes current literature examining the effect of bark beetles on burn severity, with specific attention to location, time since outbreak, and their definition of severity. There are many more studies using field data to model severity (e.g., Page and Jenkins, 2007; Schoennagel et al., 2012; Simard et al., 2011), but this review was limited to studies making observations of wildfire effects.

Table 2.1: Recent research examining the effect of bark beetle induced tree mortality on burn severity.

Reference	Location	Time since Outbreak	Definition of Burn Severity	Burn Severity Response
Turner et al., 1999	Greater Yellowstone Ecosystem	5-17 years	Observational assessment of soil and vegetation (*Turner et al.* Table 1)	Decreased then increased at higher beetle intensity
Bigler et al., 2005	Colorado	~60 years	dNBR	Increased
Kulakowski and Veblen, 2007	Colorado	0-5 years	dNBR	No effect
Bond et al., 2009	Southern California	0-1 years	RdNBR	No effect
Kulakowski and Jarvis, 2011	Colorado and Wyoming	Variable	Undefined	No effect
(Harvey et al., 2014a)	Greater Yellowstone Ecosystem	0-3 years; 3-15 years	Char height/bole scorch, tree-mortality, depth and char of post-fire litter	Variable, increased (0-3 years), no effect (3-15 years)
(Harvey et al., 2014b)	Northern Rocky Mountains	0-2 years; 3-10 years	Char height/bole scorch, tree-mortality, depth and char of post-fire litter	Variable, mostly no effect
Prichard and Kennedy, 2014	Washington	0-3 years	RdNBR	Increased
Agne et al., 2016	Oregon	8-15 years*	CBI, char height, basal area killed, crown consumed, depth and char of post-fire litter	Decreased
Meigs et al., 2016	Washington and Oregon	Variable	RdNBR	Decreased
McCarley et al. (*This Study*)	Oregon	6-12 years*	LiDAR-estimated change in canopy cover	Increased

* Differences in reported time since outbreak for the same fire (Pole Creek) were due to Agne et al. (2016) using the year of epidemic initiation at their study plots (Michelle Agne, Oregon State University, Corvallis, Oregon, USA, personal communication), while McCarley et al. (*This Study*) reported time since outbreak using the peak period of mortality across the LiDAR acquisition area (Appendix C).

Studies examining relationships between antecedent forest treatments and burn severity have similar limitations. Many are based on theoretical fire behavior (Finney, 2001; Stephens & Moghaddas, 2005; Stephens et al., 2009; van Wagtendonk, 1996), while those observing fire effects in the field are based on a finite number of sampling plots rather than landscape scale synoptic

measurements (Kennedy & Johnson, 2014; Moghaddas & Craggs, 2007; Pollet & Omi, 2002; Prichard et al., 2010; Ritchie et al., 2007; Safford et al., 2009, 2012; Strom & Fulé, 2007). These studies also face a common challenge inherent to fire ecology: the lack of pre-fire data. Few field studies have measurements of treated and untreated stands before and after a fire (Raymond & Peterson, 2005), and those that do rely on the assumption that their plots represent the range of heterogeneity in severity seen across the fire. When landscape scale severity has been measured, only unitless spectral indices (i.e., dNBR or RdNBR), sometimes validated using CBI (another index), have been used (Finney, McHugh, & Grenfell, 2005; Prichard & Kennedy, 2014; van Leeuwen, 2008; Wimberly et al., 2009).

To-date, no prior study has quantified specific, biometric effects of wildfire on forests following MPB-induced tree mortality or forest treatments across an entire fire, in part because of the challenges in acquiring field observations of forest biometrics as described above. However, the recent general increase in available Light Detection and Ranging (LiDAR) data has resulted in several cases where repeat LiDAR data capture the changes effected by a wildfire over large areas, including the event analyzed here, which occurred in an forest where varying levels of extensive MPB damage and multiple timber harvest treatment types and ages were present pre-fire. LiDAR is a proven forest measurement tool, able to detect numerous structural changes in canopy height, cover, height distribution of outer canopy surfaces, vertical distribution of canopy material, volume, biomass, and gap size (Hudak et al., 2009; Kane et al., 2013; Lefsky et al., 2002). Following the 2012 Pole Creek Fire in central Oregon, post-fire LiDAR data was acquired in 2013 to resample an area flown in 2009 following an extensive MPB outbreak in the early 2000s. Using these data, McCarley et al. (*Chapter 1*, this thesis) explored empirical relationships between spectral indices derived from Landsat and landscape-scale measurements of forest structure change by LiDAR. They found that change in canopy cover was the most accurately predicted fire effect and that a multi-temporal band ratio (d74)

outperformed other more widely utilized indices (i.e., dNBR and RdNBR). However, they also noted anomalous patterns in their data that were spatially coincident with pre-fire tree mortality from MPB-induced tree mortality and forest harvest. Since the McCarley et al. (*Chapter 1*, this thesis) analysis did not explore the specific impacts of pre-fire disturbances on model relationships, their results raise significant questions regarding the influence of MPB and forest harvest on both model accuracy and subsequent fire effects.

The objective of this study was to determine the influence of antecedent MPB outbreak and forest harvest treatments on subsequent fire severity. This study quantifies this effect by evaluating change in canopy cover (dCC) as estimated by multi-temporal LiDAR for areas identified as being affected by (1) MPB followed by wildfire (MPB/Fire), (2) harvest followed by wildfire (HARV/Fire), (3) a combination of forest harvest and MPB followed by fire (HARV/MPB/Fire), and (4) wildfire having not been proceeded by either MPB or harvest (Fire-only). Areas outside of the fire affected by (5) MPB, (6) HARV, (7) HARV/MPB, and (8) no pre-fire agent (No Agent/No Fire) were quantified as a control. In addition to analyzing these differences, this study also sought to understand how MPB outbreak intensity, harvest treatment type, and time since forest harvest treatment affected severity by exploring trends in these attributes.

2. Material and Methods

2.1. Study Area

The Pole Creek Fire (10,800 ha) occurred in September 2012 in the eastern Cascade Mountains of central Oregon (Fig. 2.1). One-third of the fire area falls within the Three Sister's Wilderness Area. Of the remaining two-thirds, timber harvest is allowed on 3,403 hectares and another 2,536 hectares with scenic view restrictions. MPB caused significant mortality, especially

throughout the wilderness area, between 2000 and 2006 (Appendix C). For additional description of the study area, see McCarley et al. (*Chapter 1*, this thesis).

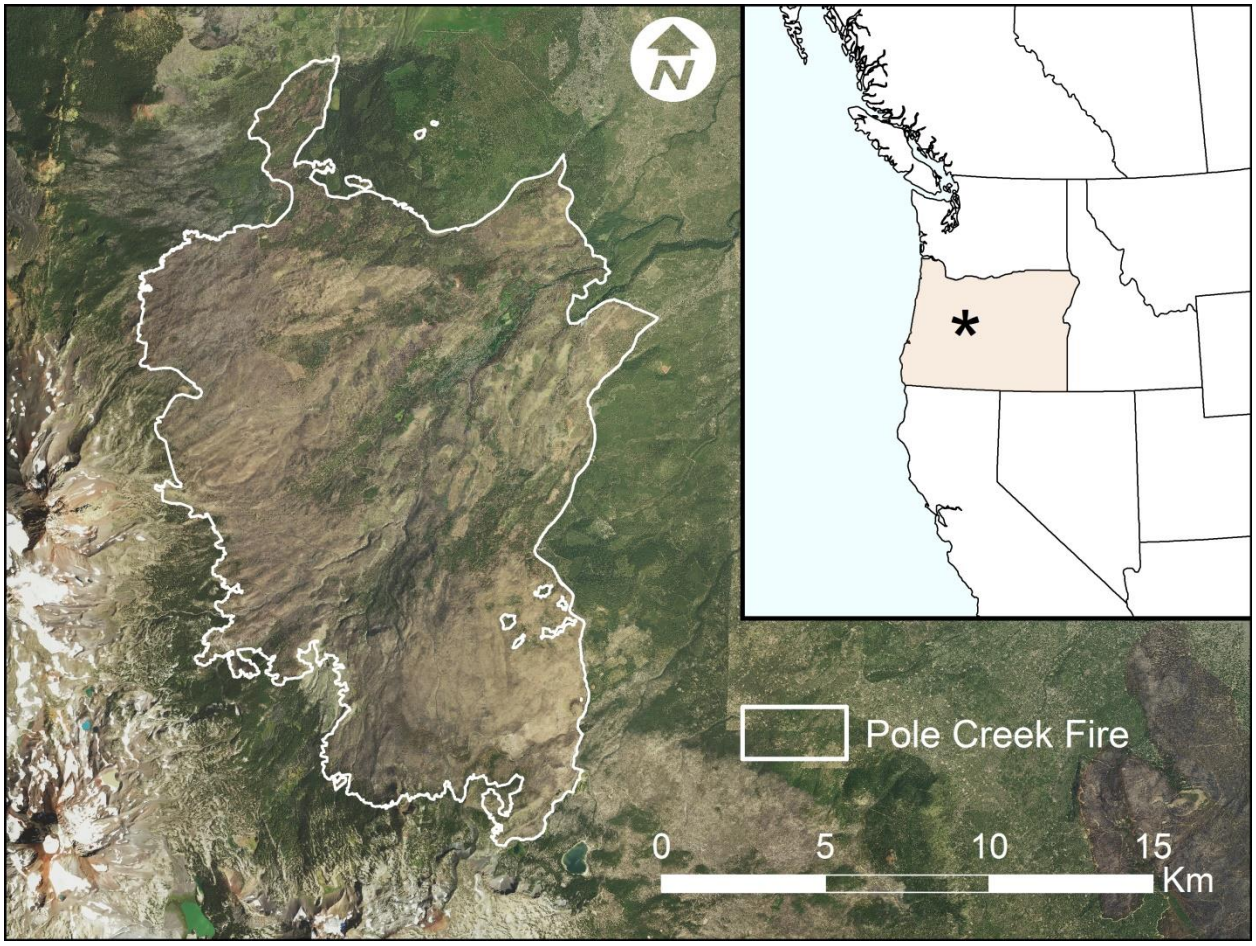

Figure 2.1: Location of Pole Creek Fire (white outline) in central Oregon. Data overlaid on 2014 National Agriculture Imagery Program imagery.

2.2 LiDAR Data

Pre- and post-fire LiDAR data available across the entire fire were processed and transformed to a 30-meter grid representing estimated dCC as described in McCarley et al. (*Chapter 1*, this thesis).

2.3. MPB Data

Aerial detection survey (ADS) data was acquired from the USDA Forest Service Pacific Northwest Region and converted mortality estimates into trees per hectare (TPH). Preliminary analysis of the ADS data showed that peak mortality occurred between 2000 and 2006 (Appendix C); therefore, the sampled data was limited to those years. ADS polygons were converted into 30-meter gridded data such that the output raster cells aligned with those of the 30-meter LiDAR-derived dCC raster. However, polygons are sketched at a map-scale between 1:250,000 and 1:50,000 depending on the flight (McConnel, Johnson, & Burns, 2000), meaning the distance between two Landsat pixels could be as little as 0.12 centimeters on paper. The unit of observation, and thus effective minimum mapping unit according to some sources, is 0.4 hectares (Johnson & Ross, 2008). Due to the noise in the original ADS data, a 3x3 moving window was applied to smooth the mortality estimates. Subsequent testing showed that the 3x3 filtered data yielded better results than the uncorrected 30-meter ADS data. Finally, TPH estimates were summed over the seven-year window from 2000-2006 to produce cumulative MPB mortality (Fig. 2.2).

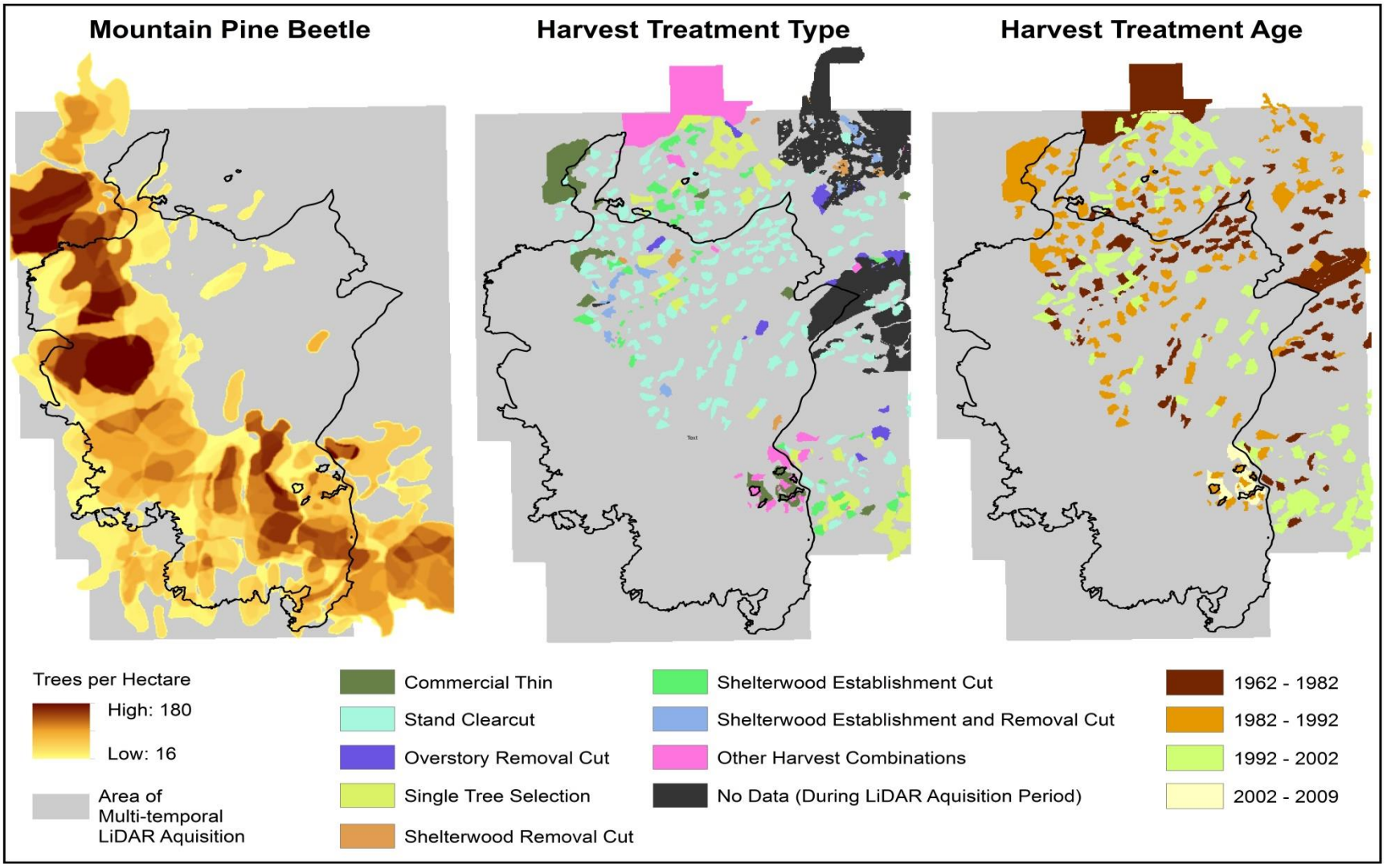

Figure 2.2: (Left) Cumulative area affected by mountain pine beetle reported by areal detection survey data between 2000 and 2006 (peak outbreak years). Harvest treatment types (Center) and treatment age (Right) reported by the Deschutes National Forest.

Multiple sources have suggested that ADS data give only rough estimates of mortality (McConnel et al., 2000; Meddens, Hicke, & Ferguson, 2012; Meigs, Kennedy, & Cohen, 2011). This study also recognized that at relatively low TPH values, MPB–induced tree mortality is indistinguishable from background levels from other causes of mortality (i.e., disease, wind throw, drought). During analysis for McCarley et al. (*Chapter 1*, this thesis), changes in the ability of spectral indices to model LiDAR-estimated dCC were observed at different TPH levels. Expanding on this finding, ordinary least squares (OLS) regressions were developed between three spectral indices, chosen for their dominance in the literature and performance in McCarley et al. (*Chapter 1*, this thesis), and change in canopy cover for Fire-only areas. Model performance was then evaluated across varying TPH thresholds (determining which areas to include in Fire-only), looking for changes in r-squared values that would indicate the limit of MPB influence. Use of the 'segmented' package (Muggeo, 2008) in R (R Development Core Team, 2014) allowed for quantification of specific breakpoints (Appendix D). The common breakpoint for all indices was near 16 TPH, only 4 TPH higher than the threshold used in similar work to isolate epidemic MPB outbreak (Agne et al., 2016). For the remainder of the analysis MPB-affected areas were defined as those with impacts above background noise (>16 TPH).

2.4. Forest Treatment Data

Forest harvest activity history was provided by the Deschutes National Forest, which has spatial records of harvest and fuel reduction activities dating back to the 1960s (Fig. 2.2). Inside the fire perimeter, 10 unique combinations of forest treatments were identified. These include stand clearcut (570 ha); single tree selection (70 ha); commercial thin (47 ha); a combination of shelterwood establishment and removal cut (40 ha); overstory removal cut (29 ha); shelterwood removal cut (28 ha); shelterwood establishment cut (19 ha); a combination of pre-commercial thin,

commercial thin, and pile burning (6 ha); two-aged seed-tree and removal cut (4 ha); and two-aged coppice cut (3 ha).

Areas where forest treatments occurred after the pre-fire LiDAR acquisition date in 2009 (1,187 ha total; 137 ha inside the fire perimeter) were excluded from the analysis. Timing of the most recent treatments inside the fire varied, the most recent being pile burning in 2006 and the oldest being overstory removal cutting in 1971. Activity age outside the fire ranged from 1962 through 2008. Treatment age was classified broadly using decades prior to fire: 2002-2012 (9 ha), 1992-2002 (251 ha), 1982-1992 (307 ha), and pre-1982 (250 ha).

2.5. Analysis

This study evaluated the effect of MPB and timber harvest on LiDAR-estimated dCC by comparing the distributions for possible combinations of disturbances (Fig. 2.3): MPB/Fire, HARV/Fire, HARV/MPB/Fire, Fire-only, MPB, HARV, HARV/MPB, and No Agent/No Fire (i.e., control). Due to the large sample size, tests of significance (i.e., ANOVA) were excessively sensitive to differences between the groups (i.e., all differences are significant), so this study instead describes the differences and reports median value ($\tilde{x}$) and interquartile range (IQR) for each distribution. The effect of MPB and timber harvest was further explored by repeating this analysis across harvest types and at increasing levels of pre-fire beetle mortality. Due to the uncertainty associated with ADS mortality estimates, MPB impacts were binned into 24 TPH increments using the range from greater than 16 TPH to the maximum observed cumulative TPH (183). The results visualize the distribution of dCC values for the binned TPH groups, and compare these to HARV/Fire and Fire-only areas. Forest treatment activities were separated by type, excluding two-aged coppice cut, two-aged seed-tree and removal cut, and the combination of pre-commercial thin, commercial thin, and pile burning; as these areas were deemed too small to be representative (3 ha, 4 ha, and 6 ha, respectively). The

distributions of the different timber harvest types were compared with each other and MPB/Fire and Fire-only pixel distributions, looking for trends in severity caused by harvest type. Finally, the distribution of the four harvest-age classes were plotted to evaluate trends in severity resulting from time since harvest.

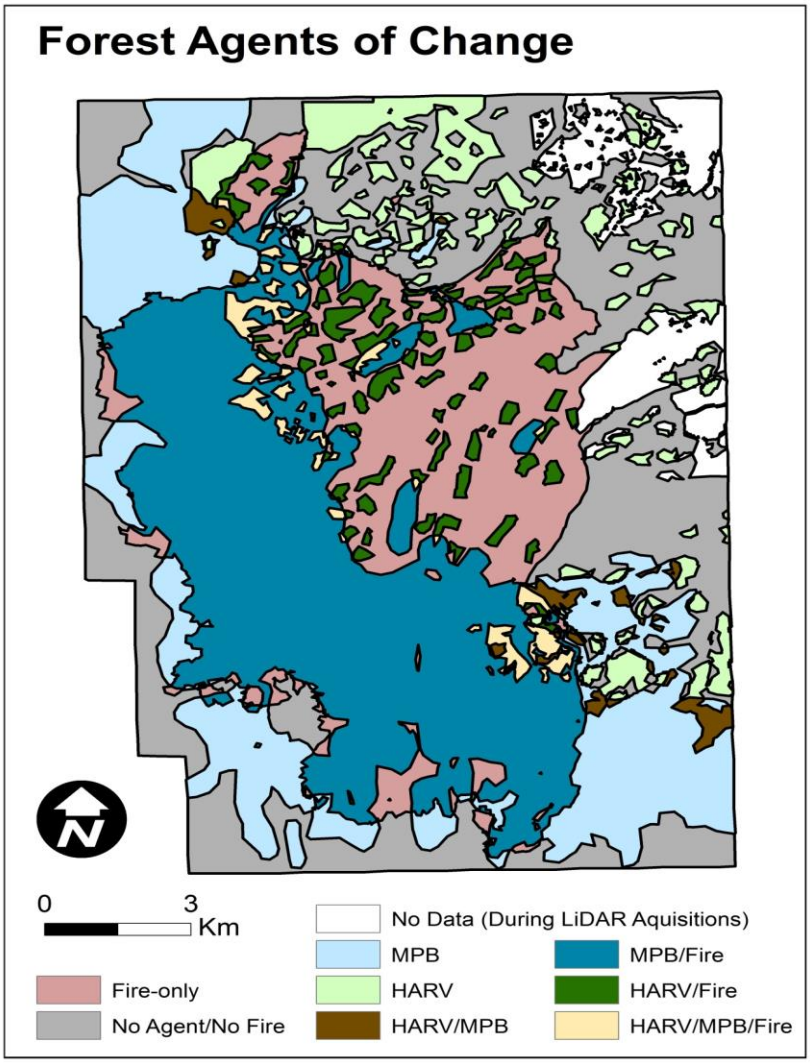

Figure 2.3: Possible combinations of forest agents of change represented in the study: Mountain pine beetle (MPB) followed by wildfire (MPB/Fire), harvest followed by wildfire (HARV/Fire), a combination of forest harvest and MPB followed by fire (HARV/MPB/Fire), wildfire having not been proceeded by either MPB or harvest (Fire-only); and areas outside of the fire affected by MPB, HARV, HARV/MPB, and no pre-fire agent (No Agent/No Fire).

3. Results

Exploring burn severity as measured by LiDAR-estimated change in canopy cover, there were noticeable differences in the median values between the pre-fire agents of change (Table 2.2 & Fig. 2.4). All areas experiencing fire showed higher severity than areas not experiencing fire. Considering the areas within the fire perimeter, those experiencing pre-fire MPB mortality had the highest severity (MPB/Fire), followed by Fire-only areas, HARV/Fire, and finally areas HARV/MPB/Fire. In addition to observing higher severity in MPB/Fire than HARV/Fire or Fire-only, burn severity increased with MPB outbreak intensity (Table 2.3 & Fig. 2.5).

Table 2.2: Descriptive statistics for possible combinations of forest agents.

Change agents	**Size (ha)**	**Median (Δ%CC)***	**IQR (Δ%CC)***
MPB/Fire	6,055	18.8	8.8 – 32.2
Fire-only	3,332	11.1	4.9 – 21.6
HARV/Fire	816	3.9	-0.1 – 11.6
HARV/MPB/Fire	411	2.1	-1.0 – 7.1
MPB	3,067	1.0	-1.0 – 3.7
No Agent/No Fire	5,225	0.1	-1.6 – 2.2
HARV	1,460	-1.2	-3.5 – 1.4
HARV/MPB	281	-1.4	-4.3 – 1.3

* Change in percent canopy cover estimated by LiDAR = Δ%CC

Table 2.3: Descriptive statistics for levels of mountain pine beetle (MPB) intensity.

MPB Intensity (Trees per Hectare (TPH))	**Size (ha)**	**Median (Δ%CC)***	**IQR (Δ%CC)***
16 – 40	1,436	11.6	5.3 – 24.0
40 – 64	1,283	17.7	8.4 – 31.9
64 – 88	1,249	22.3	10.9 – 33.8
88 – 112	874	22.7	11.4 – 34.8
112 – 136	779	19.3	9.6 – 32.5
136 – 160	316	25.1	14.9 – 34.2
160 – 183	119	33.0	27.2 – 39.2

* Change in percent canopy cover estimated by LiDAR = Δ%CC

Results indicated lower severity in timber harvest treatments than in MPB or Fire-only, with little variation between treatment types (Table 2.4 & Fig. 2.6). The lowest average severities occurred in shelterwood removal cuts, followed by commercial thinning, single tree selection, shelterwood establishment cuts, and overhead removal cuts. The highest severities were in stand clearcuts and the combination of shelterwood establishment and removal cuts. Time since treatment had a small effect on severity (Table 2.5 & Fig. 2.7), with relatively higher severity for treatments between 1971 and 1982 and little difference for more recent activities: 1982 to 1992, 1992 to 2002, and 2002 until the first LiDAR acquisition in 2009.

Table 2.3: Descriptive statistics for harvest treatment type.

Harvest Treatment Type	**Size (ha)**	**Median (Δ%CC)***	**IQR (Δ%CC)***
Shelterwood Establishment and Removal Cut	40	7.7	3.2 – 16.0
Stand Clearcut	570	5.0	0.0 – 13.5
Overhead Removal Cut	29	2.6	0.3 – 5.6
Shelterwood Establishment Cut	19	2.5	-1.0 – 6.6
Single Tree Selection Cut	70	1.9	-1.2 – 5.6
Commercial Thinning	47	1.7	-0.8 – 7.1
Shelterwood Removal Cut	28	0.1	-1.8 – 3.2

* Change in percent canopy cover estimated by LiDAR = Δ%CC

Table 2.3: Descriptive statistics for harvest treatment age.

Harvest Treatment Age	**Size (ha)**	**Median (Δ%CC)***	**IQR (Δ%CC)***
1971 – 1982	250	6.7	1.5 – 14.4
1982 – 1992	307	2.4	-1.2 – 9.5
1992 – 2002	251	3.5	-0.1 – 10.1
2002 – 2009	9	2.4	0.6 – 4.8

* Change in percent canopy cover estimated by LiDAR = Δ%CC

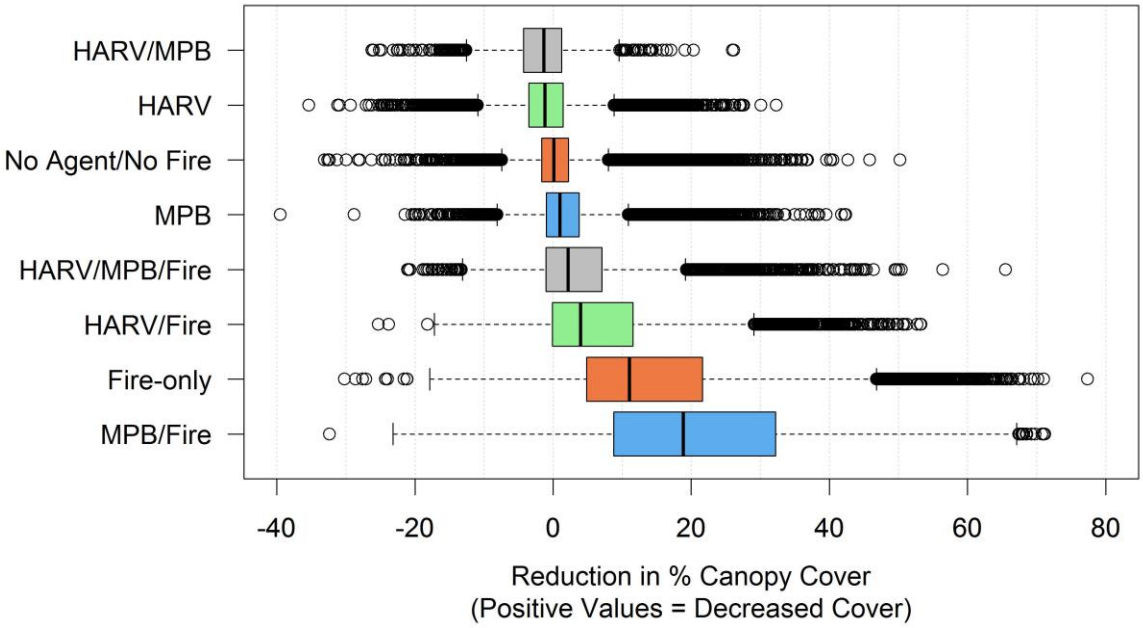

Figure 2.4: Distribution of change in percent canopy cover for possible combinations of agents: timber harvest and mountain pine beetle (HARV/MPB), HARV, No Agent/No Fire, MPB, timber harvest and mountain pine beetle followed by fire (HARV/MPB/Fire), HARV/Fire, Fire-only, and MPB/Fire. Solid lines represent medians, boxes show the interquartile range, whiskers extend to 1.5 times the interquartile range, and points are outliers.

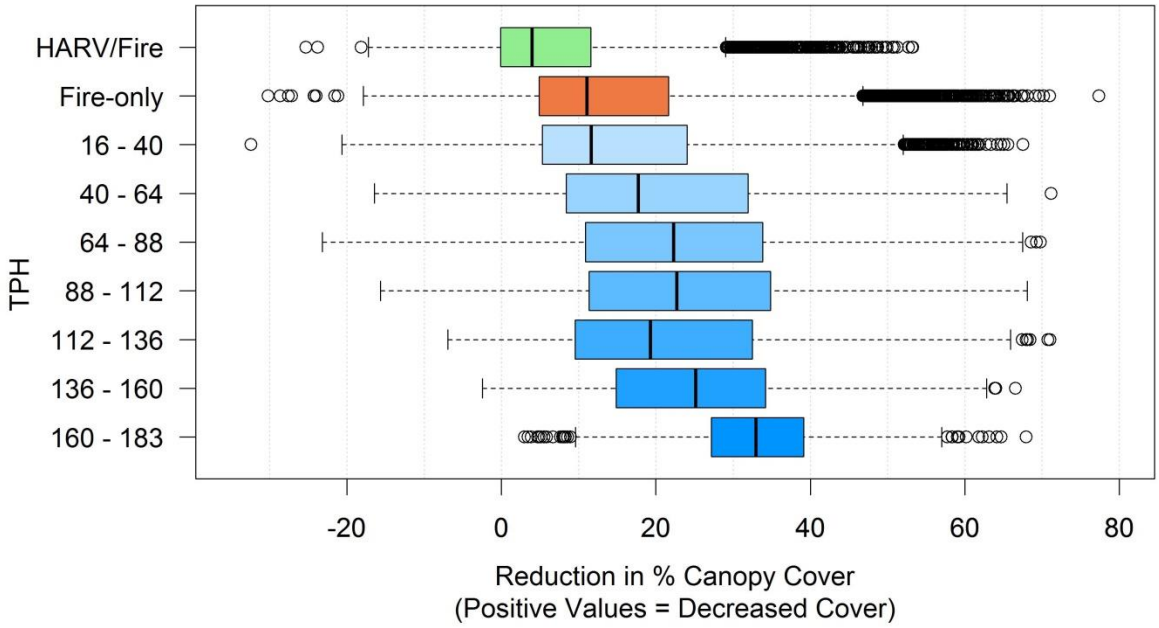

Figure 2.5: Distributions of change in percent canopy cover for timber harvest followed by wildfire (HARV/Fire), Fire-only, and cumulative MPB-induced mortality binned at 24 trees per hectare (TPH). Solid lines represent the medians, boxes show the interquartile range, whiskers extend to 1.5 times the interquartile range, and points are outliers.

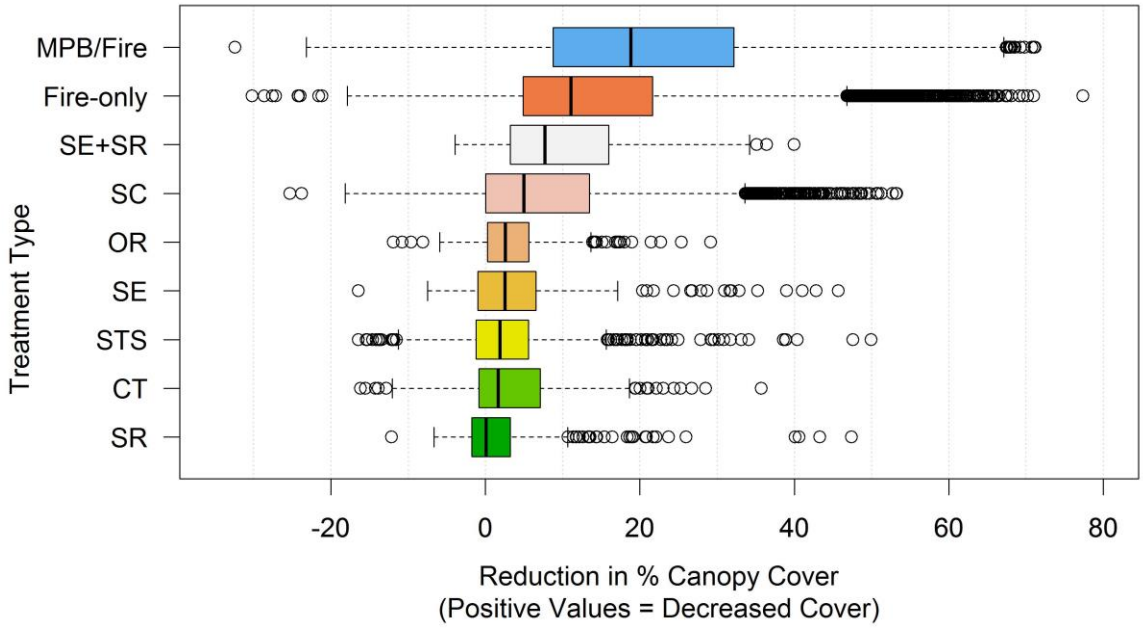

Figure 2.6. Distributions of change in percent canopy cover for mountain pine beetle followed by wildfire (MPB/Fire), Fire-only, and harvest treatment types: combination of Shelterwood Establishment and Removal Cut (SE+SR), Stand Clearcut (SC), Overstory Removal Cut (OR), Shelterwood Establishment Cut (SE), Single Tree Selection (STS), Commercial Thin (CT), and Shelterwood Removal Cut (SR). Solid lines represent the medians, boxes show the interquartile range, whiskers extend to 1.5 times the interquartile range, and points are outliers.

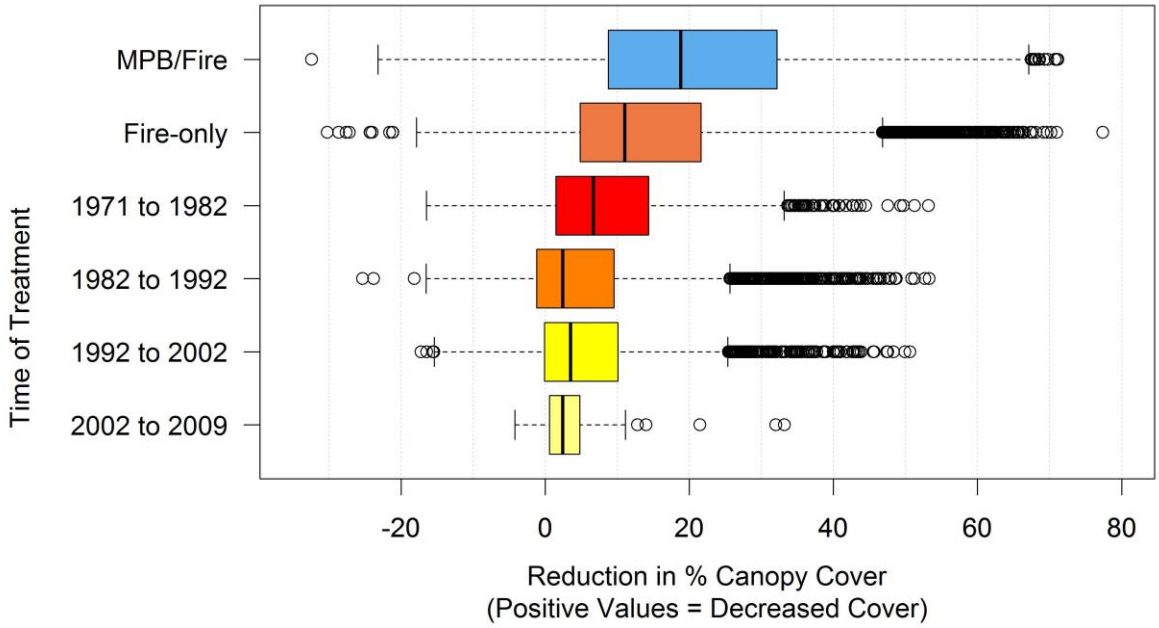

Figure 2.7: Distributions of change in percent canopy cover for mountain pine beetle followed by wildfire (MPB/Fire), Fire-only, and harvest treatment age binned by decades before fire. Solid lines represent the medians, boxes show the interquartile range, whiskers extend to 1.5 times the interquartile range, and points are outliers.

4. Discussion

4.1. Effect of MPB

This study observed higher average burn severities in areas of antecedent MPB tree mortality than in areas unaffected or with background levels of mortality (TPH ≤ 16). Areas experiencing only MPB (i.e., no fire) had greater reductions in canopy cover than other agent combinations outside the fire perimeter, suggesting some of the observed effect could be post-MPB snag fall. However, the change in canopy cover was significantly below that of MPB/Fire and also below the other agent combinations within the fire perimeter.

A positive relationship was noted between MPB intensity and subsequent burn severity (defined here as the reduction in estimated percent canopy cover). This trend was observed even

when normalizing for stand density by using change in canopy cover as a percent of pre-fire LiDAR canopy returns (Fig. 2.8). These results agree with several prior studies (Table 2.1); however, the definition of severity, time since outbreak, and method of identifying beetle impacts varied significantly in these studies. One notable difference was time since outbreak, as Prichard and Kennedy (2014) and Harvey et al. (2014a) found higher severities only in recently affected stands (0-3 years since attack), which diverge considerably in structure and flammability from the stands observed by this study due to needle retention (Hicke et al., 2012; Jolly et al., 2012). Meanwhile, Bigler et al. (2005) evaluated stands at much older post-outbreak stage (~60 years), well into the period of snag-fall and regrowth (Hicke et al., 2012) and beyond what other studies have directly measured (Donato, Harvey, Romme, Simard, & Turner, 2013; Schoennagel et al., 2012).

The results of this study diverge from studies finding decreased or no effect from antecedent MPB on burn severity (Table 2.1). This section focuses on two of the most recent studies that are of interest because of their coincident location. Agne et al. (2016) established and evaluated burn severity at 52 plots within the Pole Creek fire. They found that their measures of physical burn severity (bole char height, proportion of canopy consumed, basal area killed, soil char depth, and proportion of ground char) and CBI estimates decreased with increasing MPB effect. Meigs et al. (2016) evaluated fires across Oregon and Washington, narrowly excluding the Pole Creek fire due to the time period of analysis. They also observed decreased fire severity (defined as RdNBR) in areas affected by MPB. Certainly, some of the disagreement in both these cases is due to different measures of severity, especially when comparing canopy vegetation and soil effects. However, other measures of severity such as proportion of canopy consumed are similar to this studies' severity measurement, leading to uncertainty as to the nature of the difference in results.

The use of multi-temporal LiDAR improves on these studies in several important ways. While Agne et al. (2016) used some quantitative, well-defined measures of burn severity, they lacked

pre-fire data. This leads to uncertainty about the accuracy of attributing changes observed post-fire, to either fire or MPB (Roy et al., 2013; Smith et al., 2016, 2010). Also, because they established a relatively small number of plots, Agne et al. (2016) may not have been able to capture the same range of heterogeneity in effects observed by LiDAR over the entire fire. Using multi-temporal reflectance data (RdNBR), Meigs et al. (2016) were better able to capture the change at a landscape-scale; although, there are considerable issues arising from the use of spectral indices alone as a measure of severity. Other studies have already indicated many of these shortcomings (Kolden et al., 2015; Lentile et al., 2009; Roy et al., 2006; Smith et al., 2016). However, this study uncovered further cause for concern in the abnormal trends noticed when correlating RdNBR to LiDAR metrics. Specifically, in areas affected by MPB pre-fire NBR values near zero, combined with negative post-fire NBR values related to the fire, cause the RdNBR equation to produce unreasonably high values (between 2,000 and 18,200), as was noted by Parks et al. (2014). It is doubtful that these higher levels of severity can be meaningfully compared to RdNBR values falling within the normal range (below 2,000). This study observed clear evidence that these anomalous severity values are related to MPB through both spatial coincidence and quantification of the error, showing more area being affected at higher levels of MPB-induced mortality (Fig. 2.9). Given these limitations, this study presents a valid challenge to previous findings of no effect or decreasing burn severity following an MPB outbreak.

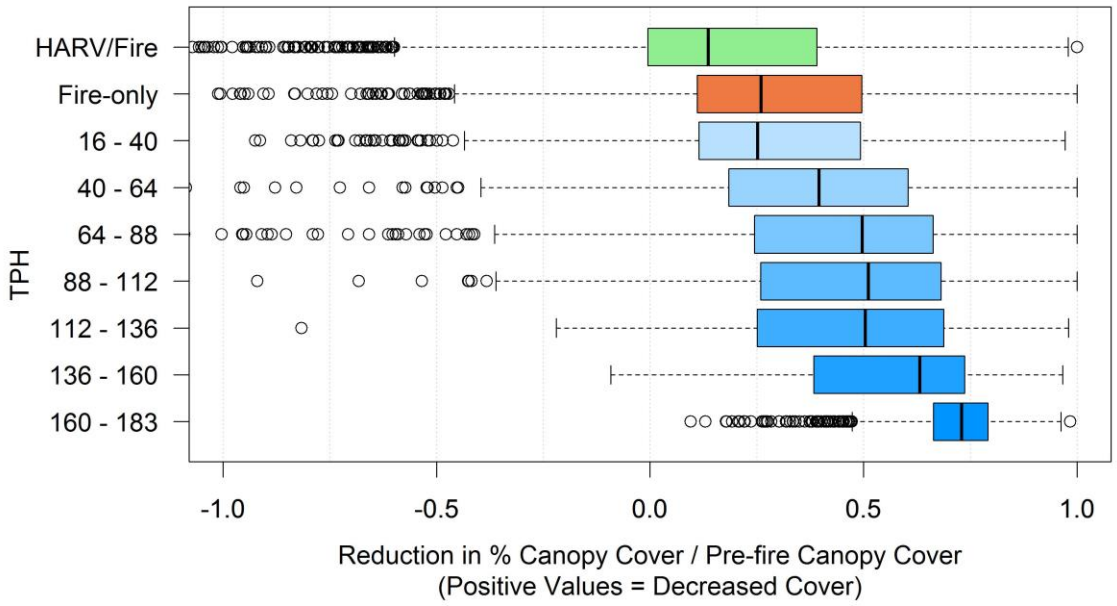

Figure 2.8: Distributions of relative change in percent canopy cover; adapted from parameters in Fig. 2.5. Extremely negative outliers not shown.

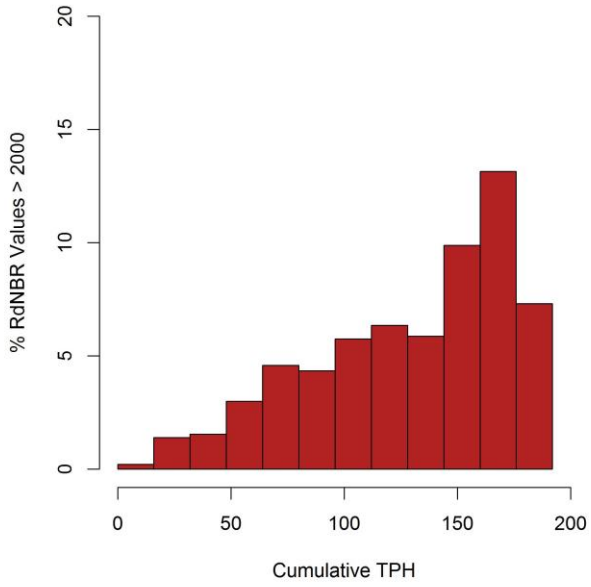

Figure 2.9: Percent of anomalous RdNBR values (> 2,000) as a percent of all RdNBR for binned cumulative trees per hectare (TPH).

4.2. Effect of Timber Harvest

The results indicate lower burn severity in timber harvest treatment activity areas, compared with areas experiencing pre-fire MPB or fire-only. Outside the fire perimeter timber harvest tended to correspond with a slight increase in canopy cover, consistent with expected growth in these areas. Finding lower burn severity in treated stands is consistent with previous research, which has modeled or observed a reduction in severity corresponding with fewer fuels (Hudak et al., 2011). However, this study explores a new method for understanding this question by improving on others' limitations. Prior work on fuel treatment reduction and wildfire severity has generally fallen into three categories. The first are studies modeling fire behavior following empirical observation of fuel treatments (Finney, 2001; Stephens et al., 2009; van Wagtendonk, 1996). These studies are particularly limited because there is no empirical observation of fire effects (because there was no actual fire). They provide impetus for experimentation and observation, but provide less significant evidence on their own. The second category is studies collecting opportunistic post-fire empirical observations in places where wildfire has burned over fuel treatments (Kennedy & Johnson, 2014; Moghaddas & Craggs, 2007; Pollet & Omi, 2002; Prichard et al., 2010; Ritchie et al., 2007; Safford et al., 2009, 2012; Strom & Fulé, 2007). In these instances, findings are limited by lack of pre-fire data, introducing significant uncertainty into accurate capture of changes caused by the fire. Additionally, they are limited to a finite number of plots, which then have to be scaled-up to make inferences across the landscape, thereby extrapolating errors. The third category of prior research on fuel treatments effect on wildfire severity is studies making empirical pre- and post-fire observations. These studies are more robust than using theoretical fire behavior or limiting work to post-fire measurements and inferences only; however, this type of work has thus far been limited in two significant ways. Either observations are based on very small treatment areas (Raymond & Peterson, 2005), leading to uncertainty at the landscape level, or they use spectral reflectance (i.e., dNBR or RdNBR) (Finney et al., 2005; Prichard

& Kennedy, 2014; van Leeuwen, 2008; Wimberly et al., 2009) unrelated to specific biometric definitions of burn severity. This study demonstrates that fuel treatments are effective at reducing burn severity, as defined by reduction in canopy, while addressing these important shortcomings of past research.

This was a unique opportunity, as no known studies have evaluated as many treatment types for the same fire. Results did not indicate major differences between most treatments, although the combination of shelterwood establishment and removal cuts and stand clearcuts had noticeably higher severities than other types. This is likely the result of time since treatment, as the oldest treatments (occurring 1971-1982) were comprised of the three treatment types with the highest severity (combination of shelterwood establishment and removal cuts, stand clearcuts, and overhead removal cuts).

There is considerable interest in understanding how time-elapsed since fuel treatment affects fire behavior, but there has been little research in this area, particularly across multiple treatment ages and types on a single fire. Some studies have attempted to model trajectories in severity for treated and untreated areas, suggesting several decades of reduced severity (Stephens, Collins, & Roller, 2012; Strom & Fulé, 2007). Using spectral remote sensing, Finney et al. (2005) demonstrated evidence of this theory for prescribed burning 1-9 years before the wildfire, while Prichard and Kennedy (2014) showed only weak correlation between treatment age and severity for treatments up to 30 years old. This study represented a unique opportunity to evaluate a wide range of treatment types occurring in a managed forest across a longer period (41 years).

The results indicate that older treatments tended to burn more severely. The oldest treatment class (1971-1982) had the highest burn severity, but still not as high as Fire-only or MPB/Fire. Among treatments that are more recent (less than 30 years), no notable difference was observed in severity, suggesting that in this ecosystem many decades are needed to accumulate surface and ladder

fuels that would lead to a fire that would produce greater canopy consumption. However, the lack of differences might also suggest unaccounted for variability in forest treatment type or burning conditions. These results are consistent with previous work suggesting managed areas burn more severely over time (Finney et al., 2005; Stephens et al., 2012; Strom & Fulé, 2007).

4.3. Effect of Harvest / MPB Combination

The results of this study show that the combined effect of MPB and timber harvest produced the lowest burn severity of any tested. This agent combination also tended to result in the greatest increase in canopy cover (i.e., forest growth) outside the fire perimeter. This study could not accurately quantify the contribution each agent has in reducing burn severity, although the other results suggest that timber harvest may be the primary driver since MPB alone tended to increase severity. This could indicate that timber harvest in post-MPB epidemic areas could reduce future burn severity. However, this implication is contingent on an accurate understanding of how MPB affects burn severity, for which there is still widespread disagreement in the literature (Hicke et al., 2012).

4.4. Uncertainties and Future Work

Certain key questions remain regarding the finding that increased severity in MPB-affected forests; in particular, the uncertainties tied to the MPB dataset. The ADS measure of mortality is based off of the number of observed trees divided by the area of the polygon mortality was observed in (McConnel et al., 2000), and is thus insensitive to stocking rate. It is possible that higher TPH values are also indicative of denser stands, which are more likely to burn at higher severity already (Agee & Skinner, 2005). However, while stocking rates might affect the increased severity observed at higher TPH levels, this does not fully explain the higher average severities in MPB/Fire even at low TPH levels compared to HARV/Fire or Fire-only. This study also noted that normalization of

change in canopy cover with pre-fire cover did not alter the findings (Fig. 2.8). Another issue that Prichard and Kennedy (2014) also discussed is that the MPB outbreak occurred primarily in Lodgepole Pine (*Pinus contorta*), which is known to be prone to higher severity fires (Agee, 1993). Since there were no homogenous stands of unaffected *P. contorta* (McCarley et al. *Chapter 1*, this thesis), the effect of MPB from the characteristics of the vegetation could not be separated.

These reservations highlight the criticality of using accurate MPB mortality estimates in future work. Other studies have produced alternatives (Prichard & Kennedy, 2014) or developed methodologies that apply corrections to ADS data. Meddens et al. (2012) developed a method of adjusting ADS data using species-specific crown area, albeit at a much coarser resolution (1 km) than would be useful for this analysis. LandTrendr (Kennedy, Yang, & Cohen, 2010) is an another useful approach, which has demonstrated effectiveness for detecting insect damage at a 30-meter resolution (Meigs, Kennedy, Gray, & Gregory, 2015). However, the use of this product was beyond the scope of the study.

Another improvement might be the use of LiDAR intensity values to separate live and dead returns. This technique has demonstrated effectiveness in other post-fire environments (Kim et al., 2009; Wing et al., 2015) and for other post-MPB outbreak forests (Bright, Hudak, Kennedy, & Meddens, 2014; Bright, Hudak, McGaughey, Andersen, & Negrón, 2013), and could shed light on what type of consumption (i.e., live or dead material) was observed in this study. Such analysis would be immensely useful in understanding remaining knowledge gaps regarding the combined effects of MPB and wildfire.

This study did not provide compelling evidence of differences in reduction of burn severity for various harvest treatment activities, although time since treatment appeared to play a significant role. This finding is consistent with the literature, but is supported only by evidence from a single fire.

The significance of time since treatment is not well understood across ecosystems that exhibit strikingly different successional characteristics. Further work in this area is warranted.

Additionally, this study examined burn severity in the canopy only. Studies observing thinning or salvage logging have shown an increase in fire severity at the ground level due to an increase in fine fuels as a result of those activities (Raymond & Peterson, 2005; Thompson, Spies, & Ganio, 2007). Given the range in definitions, caution is urged against using this study to claim broadly that burn severity is reduced by timber harvest. These results demonstrate reduced dCC as estimated by LiDAR, but additional research is needed to fully understand the complexity of burn severity throughout the ecosystem.

5. Conclusions

This study demonstrated the utility of LiDAR for understanding the effects of antecedent MPB and forest harvest treatments on subsequent burn severity, defined here as change in percent canopy cover. This marks a notable improvement over past research, which has been largely limited to observations of the post-fire environment only (i.e., no pre-fire data), or conclusions made from spectral change (i.e., dNBR and RdNBR) without biometric validation. The results indicate increased burn severity, as defined by change in LiDAR-estimated canopy cover, in areas experiencing MPB and found burn severity to increase with pre-fire MPB intensity. Conversely, harvest activities led to lower burn severity. Although harvest treatment type was not conclusively related to burn severity, time since treatment appeared to play a role, with the most recent treatments experiencing the lowest average severity. These findings show quantitative evidence that pre-fire agents of forest change are important drivers of subsequent fire effects using a specific definition of burn severity across an entire fire. This is a significant step in resolving uncertainties concerning the increasing overlap of wildfire, MPB, and forest treatments. However, considerable work in this area is still needed. Further work is

also warranted in understanding the significant limitations observed in RdNBR for areas experiencing pre-fire agents of change.

Thesis Conclusions

Chapter one explored the relationships between spectral indices calculated from Landsat imagery and changes in forest structure estimated from multi-temporal LiDAR. This chapter also showed how the use of simultaneous autoregression could improve performance by providing a proxy for other variables (i.e., geomorphic or climatic process) not in the model (Kissling & Carl, 2007; Prichard & Kennedy, 2014; Wimberly et al., 2009). The best relationship was observed between LiDAR-estimated change in canopy cover and the d74 index, followed by dNBR and dCC. In general, spectral indices were better correlated with LiDAR measures of structure higher in the vertical profile of vegetation. Similar to findings from previous work, Landsat band 7 was most sensitive to fire effects (Key & Benson, 2006; Miller & Yool, 2002; van Wagtendonk et al., 2004; White et al., 1996). The significance of this study is that it indicates the viability of calibrating spectral indices to structural measures of change, suggesting feasibility at larger scales.

Chapter two explored the impact of pre-fire MPB and forest harvest on subsequent fire-caused severity, measured by multi-temporal LiDAR estimated change in canopy cover. The results show that MPB/Fire areas had the highest burn severity, and that severity increased with pre-fire MPB intensity. Comparatively, HARV/Fire areas were associated with reduced severity. In all cases areas affected by fire showed greater change in canopy cover than areas outside the fire perimeter. Additionally, the results suggested that time since treatment affected severity, as the oldest treatments burned the most severely. The observed decrease in severity associated with timber harvest is consistent with previous research (e.g., Moghaddas & Craggs, 2007; Prichard, Peterson, & Jacobson, 2010; Ritchie, Skinner, & Hamilton, 2007; Safford, Schmidt, & Carlson, 2009; Safford, Stevens, Merriam, Meyer, & Latimer, 2012; Wimberly et al., 2009). However, uncertainty remains considering the impact of MPB outbreaks on subsequent burn severity.

Throughout this thesis, multi-temporal LiDAR exhibited considerable value in measuring fire effects across a landscape. This is significant given that few other studies have utilized this tool (Bishop et al., 2014; Reddy et al., 2015; Wang & Glenn, 2009; Wulder et al., 2009); and none across an entire fire in a forested ecosystem. Pinpointing rehabilitation needs, predicting trends in ecological recovery, mitigating secondary fire effects, and understanding forest carbon cycling are all vital tasks that require fire effects mapping (Cansler & Mckenzie, 2014; Conard et al., 2002; Eidenshink et al., 2007; Goetz et al., 2007; Hessburg et al., 2015; Hicke et al., 2003; Kashian et al., 2006; Miller, Safford, et al., 2009; Moody et al., 2008; Robichaud et al., 2009; Romme et al., 2011; Turner et al., 1994). While spectral indices are the dominant method of measuring severity across a landscape, there are numerous concerns amongst remote sensing scientists and fire ecologists (Kolden et al., 2015; Morgan et al., 2014; Roy et al., 2013, 2006; Smith et al., 2016). This work demonstrates the utility of multi-temporal LiDAR as a viable method of measuring severity, as shown in chapter two, while chapter one indicates the potential fusion of spectral indices and LiDAR metrics. This is particularly important as long as multi-temporal LiDAR datasets remain scarce. Given climatic shifts toward larger, more extreme wildfires (Barbero et al., 2015; Littell et al., 2009; Westerling et al., 2006), there has never been a greater need to monitor fire effects at the landscape level. Multi-temporal LiDAR offers a cutting-edge tool for fire ecologists to meet this challenge.

References

Agee, J. K. (1993). *Fire Ecology of Pacific Northwest Forests*. Washington, D.C.: Island Press.

Agee, J. K., & Skinner, C. N. (2005). Basic principles of forest fuel reduction treatments. *Forest Ecology and Management*, *211*(1-2), 83–96. doi:10.1016/j.foreco.2005.01.034

Agne, M. C., Woolley, T., & Fitzgerald, S. (2016). Fire severity and cumulative disturbance effects in the post-mountain pine beetle lodgepole pine forests of the Pole Creek Fire. *Forest Ecology and Management*, *366*, 73–86. doi:10.1016/j.foreco.2016.02.004

Akaike, H. (1974). A new look at the statistical model identification. *IEEE Transactions on*

Automatic Control, *19*(6), 716–723. doi:10.1109/TAC.1974.1100705

Andersen, H.-E., McGaughey, R. J., & Reutebuch, S. E. (2005). Estimating forest canopy fuel parameters using LIDAR data. *Remote Sensing of Environment*, *94*(4), 441–449. doi:10.1016/j.rse.2004.10.013

Baker, W. L. (2015). Are High-Severity Fires Burning at Much Higher Rates Recently than Historically in Dry-Forest Landscapes of the Western USA? *Plos One*, *10*(9), e0136147. doi:10.1371/journal.pone.0136147

Barbero, R., Abatzoglou, J. T., Larkin, N. K., Kolden, C. A., & Stocks, B. (2015). Climate change presents increased potential for very large fires in the contiguous United States. *International Journal of Wildland Fire*, *24*(7), 892–899. doi:10.1071/WF15083

Bater, C. W., Wulder, M. A., White, J. C., & Coops, N. C. (2010). Integration of LiDAR and digital aerial imagery for detailed estimates of lodgepole pine (Pinus contorta) volume killed by mountain pine beetle (Dendroctonus ponderosae). *Journal of Forestry*, *108*(3), 111–119.

Bigler, C., Kulakowski, D., & Veblen, T. T. (2005). Multiple disturbance interactions and drought influence fire severity in Rocky Mountain subalpine forests. *Ecology*, *86*(11), 3018–3029. doi:10.1890/05-0011

Birch, D. S., Morgan, P., Kolden, C. A., Abatzoglou, J. T., Dillon, G. K., Hudak, A. T., & Smith, A. M. S. (2015). Vegetation, topography and daily weather influenced burn severity in central Idaho and western Montana forests. *Ecosphere*, *6*(1), 1–23. doi:10.1890/ES14-00213.1

Bishop, B. D., Dietterick, B. C., White, R. A., & Mastin, T. B. (2014). Classification of plot-level fire-caused tree mortality in a redwood forest using digital orthophotography and LiDAR. *Remote Sensing*, *6*(3), 1954–1972. doi:10.3390/rs6031954

Bivand, R. (2002). Spatial econometrics functions in R: Classes and methods. *Journal of Geographical Systems*, *4*(4), 405–421. doi:10.1007/s101090300096

Bond, M. L., Lee, D. E., Bradley, C. M., & Hanson, C. T. (2009). Influence of Pre-Fire Tree Mortality on Fire Severity in Conifer Forests of the San Bernardino Mountains , California. *The Open Forest Science Journal*, *2*, 41–47.

Bright, B. C., Hicke, J. A., & Hudak, A. T. (2012). Estimating aboveground carbon stocks of a forest affected by mountain pine beetle in Idaho using lidar and multispectral imagery. *Remote Sensing of Environment*, *124*, 270–281. doi:10.1016/j.rse.2012.05.016

Bright, B. C., Hudak, A. T., Kennedy, R. E., & Meddens, A. J. H. (2014). Landsat Time Series and Lidar as Predictors of Live and Dead Basal Area Across Five Bark Beetle-Affected Forests. *IEEE Journal of Selected Topics in Applied Earth Observations and Remote Sensing*, *7*(8), 3440–3452. doi:10.1109/JSTARS.2014.2346955

Bright, B. C., Hudak, A. T., McGaughey, R., Andersen, H.-E., & Negrón, J. (2013). Predicting live and dead tree basal area of bark beetle affected forests from discrete-return lidar. *Canadian Journal of Remote Sensing*, *39*(sup1), S99–S111. doi:10.5589/m13-027

Brown, J. K., Oberhau, R. D., & Johnston, C. M. (1982). *Handbook for Inventorying surface fuels and biomass in the Interior West*. *General Technical Report INT-129*. Ogden, UT: USDA Forest Service, Intermountain Forest and Range Experiment Station (48 pp.).

Cansler, C. A., & McKenzie, D. (2012). How robust are burn severity indices when applied in a new region? Evaluation of alternate field-based and remote-sensing methods. *Remote Sensing*, *4*(2), 456–483. doi:10.3390/rs4020456

Cansler, C. A., & Mckenzie, D. (2014). Climate, fire size, and biophysical setting control fire severity and spatial pattern in the northern Cascade Range, USA. *Ecological Applications*, *24*(5), 1037–1056. doi:10.1890/13-1077.1

Chander, G., & Markham, B. (2003). Revised Landsat-5 TM Radiometrie Calibration Procedures and Postcalibration Dynamic Ranges. *IEEE Transactions on Geoscience and Remote Sensing*, *41*(11), 2674–2677. doi:10.1109/TGRS.2003.818464

Chavez, P. S. J. (1996). Image-based atmospheric corrections- revisited and improved. *Photogrammetric Engineering and Remote Sensing*, *62*(9), 1025–1035. doi:0099-1112/96/6209-1025

Chuvieco, E., Martín, M. P., & Palacios, A. (2002). Assessment of different spectral indices in the red-near-infrared spectral domain for burned land discrimination. *International Journal of Remote Sensing*, *23*(23), 5103–5110. doi:10.1080/01431160210153129

Cocke, A. E., Fulé, P. Z., & Crouse, J. E. (2005). Comparison of burn severity assessments using Differenced Normalized Burn Ratio and ground data. *International Journal of Wildland Fire*, *14*(2), 189. doi:10.1071/WF04010

Conard, S. G., Sukhinin, A. I., Stocks, B. J., Cahoon, D. R., Davidenko, E. P., & Ivanova, G. A. (2002). Determining Effects of Area Burned and Fire Severity on Carbon Cycling and Emissions in Siberia. *Climatic Change*, *55*(1), 197–211. doi:10.1023/A:1020207710195

Cressie, N. (1993). *Statistics for Spatial Data*. New York: Wiley.

Crist, E. P. (1985). A TM Tasseled Cap equivalent transformation for reflectance factor data. *Remote Sensing of Environment*, *17*(3), 301–306. doi:10.1016/0034-4257(85)90102-6

De Santis, A., & Chuvieco, E. (2009). GeoCBI: A modified version of the Composite Burn Index for the initial assessment of the short-term burn severity from remotely sensed data. *Remote Sensing of Environment*, *113*(3), 554–562. doi:10.1016/j.rse.2008.10.011

Dillon, G. K., Holden, Z. A., Morgan, P., Crimmins, M. A., Heyerdahl, E. K., & Luce, C. H. (2011). Both topography and climate affected forest and woodland burn severity in two regions of the western US, 1984 to 2006. *Ecosphere*, *2*(12), 1–33. doi:10.1890/ES11-00271.1

Disney, M. I., Lewis, P., Gomez-Dans, J., Roy, D. P., Wooster, M. J., & Lajas, D. (2011). 3D radiative transfer modelling of fire impacts on a two-layer savanna system. *Remote Sensing of Environment*, *115*(8), 1866–1881. doi:10.1016/j.rse.2011.03.010

Dixon, G. E. (2002). *Essential FVS : A User's Guide to the Forest Vegetation Simulator*. Fort Collins,

CO: USDA Forest Service, Forest Management Service Center (226 pp).

Donato, D. C., Harvey, B. J., Romme, W. H., Simard, M., & Turner, M. G. (2013). Bark beetle effects on fuel profiles across a range of stand structures in Douglas-fir forests of Greater Yellowstone. *Ecological Applications*, *23*(1), 3–20. doi:10.1890/12-0772.1

Eidenshink, J., Schwind, B., Brewer, K., Zhu, Z., Quayle, B., & Howard, S. (2007). A Project for Monitoring Trends in Burn Severity. *Fire Ecology Special Issue*, *3*(1), 3–21.

Epting, J., Verbyla, D., & Sorbel, B. (2005). Evaluation of remotely sensed indices for assessing burn severity in interior Alaska using Landsat TM and ETM+. *Remote Sensing of Environment*, *96*(3-4), 328–339. doi:10.1016/j.rse.2005.03.002

Finney, M. A. (2001). Design of regular landscape fuel treatment patterns for modifying fire growth and behavior. *Forest Science*, *47*(2), 219–228.

Finney, M. A., McHugh, C. W., & Grenfell, I. C. (2005). Stand- and landscape-level effects of prescribed burning on two Arizona wildfires. *Canadian Journal of Forest Research*, *35*(7), 1714–1722. doi:10.1139/x05-090

French, N. H. F., Kasischke, E. S., Hall, R. J., Murphy, K. A., Verbyla, D. L., Hoy, E. E., & Allen, J. L. (2008). Using Landsat data to assess fire and burn severity in the North American boreal forest region: an overview and summary of results. *International Journal of Wildland Fire*, *17*(4), 443–462. doi:10.1071/WF08007

Gao, B. C. (1996). NDWI - A normalized difference water index for remote sensing of vegetation liquid water from space. *Remote Sensing of Environment*, *58*(3), 257–266. doi:10.1016/S0034-4257(96)00067-3

Gillespie, A. J. R. (1999). Rationale for a National Annual Forest Inventory Program. *Journal of Forestry*, *97*(12), 16–20.

Goetz, S. J., Mack, M. C., Gurney, K. R., Randerson, J. T., & Houghton, R. A. (2007). Ecosystem responses to recent climate change and fire disturbance at northern high latitudes: observations and model results contrasting northern Eurasia and North America. *Environmental Research Letters*, *2*(4), 9. doi:10.1088/1748-9326/2/4/045031

Haining, R. (1990). *Spatial data analysis in the social and environmental sciences*. Cambridge: Cambridge University Press. doi:10.1017/CBO9780511623356

Harvey, B. J., Donato, D. C., Romme, W. H., & Turner, M. G. (2014a). Fire severity and tree regeneration following bark beetle outbreaks : the role of outbreak stage and burning conditions. *Ecological Applications*, *24*(7), 1608–1625.

Harvey, B. J., Donato, D. C., & Turner, M. G. (2014b). Recent mountain pine beetle outbreaks, wildfire severity, and postfire tree regeneration in the US Northern Rockies. *Proceedings of the National Academy of Sciences*, *111*(42). doi:10.1073/pnas.1411346111

Hessburg, P. F., Churchill, D. J., Larson, A. J., Haugo, R. D., Miller, C., Spies, T. A., … Reeves, G. H. (2015). Restoring fire-prone Inland Pacific landscapes: seven core principles. *Landscape*

Ecology, *30*(10), 1805–1835. doi:10.1007/s10980-015-0218-0

Hicke, J. A., Asner, G. P., Kasischke, E. S., French, N. H. F., Randerson, J. T., Collatz, G. J., … Field, C. B. (2003). Postfire response of North American boreal forest net primary productivity analyzed with satellite observations. *Global Change Biology*, *9*(8), 1145–1157. doi:10.1046/j.1365-2486.2003.00658.x

Hicke, J. A., Johnson, M. C., Hayes, J. L., & Preisler, H. K. (2012, May). Effects of bark beetle-caused tree mortality on wildfire. *Forest Ecology and Management*. Elsevier B.V. doi:10.1016/j.foreco.2012.02.005

Hicke, J. A., Meddens, A. J. H., Allen, C. D., & Kolden, C. A. (2013). Carbon stocks of trees killed by bark beetles and wildfire in the western United States. *Environmental Research Letters*, *8*, 035032. doi:10.1088/1748-9326/8/3/035032

Hicke, J. A., Meddens, A. J. H., & Kolden, C. A. (2015). Recent Tree Mortality in the Western United States from Bark Beetles and Forest Fires. *Forest Science*, *62*, 1–13.

Hoy, E. E., French, N. H. F., Turetsky, M. R., Trigg, S. N., & Kasischke, E. S. (2008). Evaluating the potential of Landsat TM/ETM+ imagery for assessing fire severity in Alaskan black spruce forests. *International Journal of Wildland Fire*, *17*(4), 500–514. doi:10.1071/WF08107

Hudak, A. T., Evans, J. S., & Smith, A. M. S. (2009). LiDAR utility for natural resource managers. *Remote Sensing*, *1*(4), 934–951. doi:10.3390/rs1040934

Hudak, A. T., Morgan, P., Bobbitt, M. J., Smith, A. M. S., Lewis, S. A., Lentile, L. B., … McKinley, R. A. (2007). The Relationship of Multispectral Satellite Imagery to Immediate Fire Effects. *Fire Ecology*, *3*(1), 64–90. doi:10.4996/fireecology.0301064

Hudak, A. T., Rickert, I., Morgan, P., Strand, E., Lewis, S. A., Robichaud, P. R., … Holden, Z. A. (2011). *Review of fuel treatment effectiveness in forests and rangelands and a case study from the 2007 megafires in central Idaho, USA. General Technican Report RMRS-GTR-252*. Fort Collins, CO: USDA Forest Service, Rocky Mountain Research Station (60 p.).

Hudak, A. T., Strand, E. K., Vierling, L. A., Byrne, J. C., Eitel, J. U. H., Martinuzzi, S., & Falkowski, M. J. (2012). Quantifying aboveground forest carbon pools and fluxes from repeat LiDAR surveys. *Remote Sensing of Environment*, *123*, 25–40. doi:10.1016/j.rse.2012.02.023

Huete, A. R. (1988). A soil-adjusted vegetation index (SAVI). *Remote Sensing of Environment*, *25*(3), 295–309. doi:10.1016/0034-4257(88)90106-X

Isenburg, M. (2013). LAStools - Efficient tools for LiDAR processing. Retrieved from http://lastools.org

Jakubauskas, M. E., Lulla, K. P., & Mausel, P. W. (1990). Assessment of vegetation change in a fire-altered forest landscape. *Photogrammetric Engineering and Remote Sensing*, *56*(3), 371–377.

Johnson, E. W., & Ross, J. (2008). Quantifying error in aerial survey data. *Australian Forestry*, *71*(3), 216–222. doi:10.1080/00049158.2008.10675038

Jolly, W. M., Parsons, R. A., Hadlow, A. M., Cohn, G. M., McAllister, S. S., Popp, J. B., … Negron, J. F. (2012). Relationships between moisture, chemistry, and ignition of Pinus contorta needles during the early stages of mountain pine beetle attack. *Forest Ecology and Management, 269*, 52–59. doi:10.1016/j.foreco.2011.12.022

Kane, V. R., Lutz, J. A., Roberts, S. L., Smith, D. F., McGaughey, R. J., Povak, N. A., & Brooks, M. L. (2013). Landscape-scale effects of fire severity on mixed-conifer and red fir forest structure in Yosemite National Park. *Forest Ecology and Management, 287*, 17–31. doi:10.1016/j.foreco.2012.08.044

Kane, V. R., North, M. P., Lutz, J. A., Churchill, D. J., Roberts, S. L., Smith, D. F., … Brooks, M. L. (2014). Assessing fire effects on forest spatial structure using a fusion of Landsat and airborne LiDAR data in Yosemite National Park. *Remote Sensing of Environment, 151*, 89–101. doi:10.1016/j.rse.2013.07.041

Kashian, D. M., Romme, W. H., Tinker, D. B., Turner, M. G., & Ryan, M. G. (2006). Carbon Storage on Landscapes with Stand-replacing Fires. *BioScience, 56*(7), 598. doi:10.1641/0006-3568(2006)56[598:CSOLWS]2.0.CO;2

Kasischke, E. S., Turetsky, M. R., Ottmar, R. D., French, N. H. F., Shetler, G., Hoy, E. E., & Kane, E. S. (2008). Evaluation of the Composite Burn Index for Assessing Fire Severity in Black Spruce Forests. *International Journal of Wildland Fire, 17*(4), 515–526. doi:10.1071/WF08002

Kauth, R. J., & Thomas, G. S. (1976). The tasselled cap - A graphic description of the spectral-temporal development of agricultural crops as seen by Landsat. In *Final Proceedings: 2nd International Symposium on Machine Processing of Remotely Sensed Data*. West Lafayette, IN: Purdue University.

Keeley, J. E. (2009). Fire intensity, fire severity and burn severity: a brief review and suggested usage. *International Journal of Wildland Fire, 18*(1), 116. doi:10.1071/WF07049

Kennedy, M. C., & Johnson, M. C. (2014). Fuel treatment prescriptions alter spatial patterns of fire severity around the wildland-urban interface during the Wallow Fire, Arizona, USA. *Forest Ecology and Management, 318*, 122–132. doi:10.1016/j.foreco.2014.01.014

Kennedy, R. E., Yang, Z., & Cohen, W. B. (2010). Detecting trends in forest disturbance and recovery using yearly Landsat time series: 1. LandTrendr — Temporal segmentation algorithms. *Remote Sensing of Environment, 114*(12), 2897–2910. doi:10.1016/j.rse.2010.07.008

Key, C. H. (2006). Ecological and Sampling Constraints on Defining Landscape Fire Severity. *Fire Ecology, 2*(2), 34–59. doi:10.4996/fireecology.0202034

Key, C. H., & Benson, N. C. (2006). Landscape Assessment (LA): Sampling and Analysis Methods. In D. C. Lutes, R. E. Keane, J. F. Caratti, C. H. Key, N. C. Benson, S. Sutherland, & L. J. Gangi (Eds.), *FIREMON: Fire effects monitoring and inventory system* (p. 51). Fort Collins, CO: USDA Forest Service General Technical Report. RMRS-GTR-164-CD.

Kim, Y., Yang, Z., Cohen, W. B., Pflugmacher, D., Lauver, C. L., & Vankat, J. L. (2009). Distinguishing between live and dead standing tree biomass on the North Rim of Grand Canyon National Park, USA using small-footprint lidar data. *Remote Sensing of Environment, 113*(11),

2499–2510. doi:10.1016/j.rse.2009.07.010

Kissling, W. D., & Carl, G. (2007). Spatial autocorrelation and the selection of simultaneous autoregressive models. *Global Ecology and Biogeography*, *17*, 59–71. doi:10.1111/j.1466-8238.2007.00334.x

Kolden, C. A., Lutz, J. A., Key, C. H., Kane, J. T., & van Wagtendonk, J. W. (2012). Mapped versus actual burned area within wildfire perimeters: Characterizing the unburned. *Forest Ecology and Management*, *286*, 38–47. doi:10.1016/j.foreco.2012.08.020

Kolden, C. A., Smith, A. M. S., & Abatzoglou, J. T. (2015). Limitations and utilisation of Monitoring Trends in Burn Severity products for assessing wildfire severity in the USA. *International Journal of Wildland Fire*, *24*(7). doi:10.1071/WF15082

Koutsias, N., & Pleniou, M. (2015). Comparing the spectral signal of burned surfaces between Landsat 7 ETM+ and Landsat 8 OLI sensors. *International Journal of Remote Sensing*, *36*(14), 3714–3732. doi:10.1080/01431161.2015.1070322

Kulakowski, D., & Jarvis, D. (2011). The influence of mountain pine beetle outbreaks and drought on severe wildfires in northwestern Colorado and southern Wyoming: A look at the past century. *Forest Ecology and Management*, *262*(9), 1686–1696. doi:10.1016/j.foreco.2011.07.016

Kulakowski, D., & Veblen, T. T. (2007). Effect of prior disturbances on the extent and severity of wildfire in Colorado subalpine forests. *Ecology*, *88*(3), 759–769. doi:10.1890/06-0124

Kushla, J. D., & Ripple, W. J. (1998). Assessing wildfire effects with Landsat thematic mapper data. *International Journal of Remote Sensing*, *19*(13), 2493–2507.

Kwak, D.-A., Chung, J., Lee, W.-K., Kafatos, M., Lee, S. Y., Cho, H.-K., & Lee, S.-H. (2010). Evaluation for Damaged Degree of Vegetation by Forest Fire using Lidar and a Digital Aerial Photograph. *Photogrammetric Engineering and Remote Sensing*, *76*(3), 277–287.

Lefsky, M. A., Cohen, W. B., Parker, G. G., & Harding, D. J. (2002). Lidar Remote Sensing for Ecosystem Studies. *BioScience*, *52*(1), 19. doi:10.1641/0006-3568(2002)052[0019:LRSFES]2.0.CO;2

Lentile, L. B., Holden, Z. A., Smith, A. M. S., Falkowski, M. J., Hudak, A. T., Morgan, P., … Benson, N. C. (2006). Remote sensing techniques to assess active fire characteristics and post-fire effects. *International Journal of Wildland Fire*, *15*(3), 319–345. doi:10.1071/WF05097

Lentile, L. B., Smith, A. M. S., Hudak, A. T., Morgan, P., Bobbitt, M. J., Lewis, S. A., & Robichaud, P. R. (2009). Remote sensing for prediction of 1-year post-fire ecosystem condition. *International Journal of Wildland Fire*, *18*(5), 594–608. doi:10.1071/WF07091

Lewis, S. A., Hudak, A. T., Ottmar, R. D., Robichaud, P. R., Lentile, L. B., Hood, S. M., … Morgan, P. (2011). Using hyperspectral imagery to estimate forest floor consumption from wildfire in boreal forests of Alaska, USA. *International Journal of Wildland Fire*, *20*(2), 255–271. doi:10.1071/WF09081

Li, F., Bond-Lamberty, B., & Levis, S. (2014). Quantifying the role of fire in the Earth system - Part

2: Impact on the net carbon balance of global terrestrial ecosystems for the 20th century. *Biogeosciences*, *11*(5), 1345–1360. doi:10.5194/bg-11-1345-2014

Littell, J. S., McKenzie, D., Peterson, D. L., & Westerling, A. L. (2009). Climate and wildfire area burned in western U . S . *Ecological Applications*, *19*(4), 1003–1021.

López-García, M. J., & Caselles, V. (1991). Mapping burns and natural reforestation using thematic Mapper data. *Geocarto International*, *6*(1), 31–37. doi:10.1080/10106049109354290

McConnel, T. J., Johnson, E. W., & Burns, B. (2000). *A Guide to Conducting Aerial sketchmapping Surveys*. Fort Collins, Colorado, USA: UDSA Forest Service, Forest Health Technology Enterprise Team, FHTET 00-01.

Meddens, A. J. H., Hicke, J. A., & Ferguson, C. A. (2012). Spatiotemporal patterns of observed bark beetle-caused tree mortality in British Columbia and the western United States. *Ecological Applications*, *22*(7), 1876–1891.

Meigs, G. W., Donato, D. C., Campbell, J. L., Martin, J. G., & Law, B. E. (2009). Forest Fire Impacts on Carbon Uptake, Storage, and Emission: The Role of Burn Severity in the Eastern Cascades, Oregon. *Ecosystems*, *12*(8), 1246–1267. doi:10.1007/s10021-009-9285-x

Meigs, G. W., Kennedy, R. E., & Cohen, W. B. (2011). A Landsat time series approach to characterize bark beetle and defoliator impacts on tree mortality and surface fuels in conifer forests. *Remote Sensing of Environment*, *115*(12), 3707–3718. doi:10.1016/j.rse.2011.09.009

Meigs, G. W., Kennedy, R. E., Gray, A. N., & Gregory, M. J. (2015). Spatiotemporal dynamics of recent mountain pine beetle and western spruce budworm outbreaks across the Pacific Northwest Region, USA. *Forest Ecology and Management*, *339*(1), 71–86. doi:10.1016/j.foreco.2014.11.030

Meigs, G. W., Turner, D. P., Ritts, W. D., Yang, Z., & Law, B. E. (2011). Landscape-Scale Simulation of Heterogeneous Fire Effects on Pyrogenic Carbon Emissions, Tree Mortality, and Net Ecosystem Production. *Ecosystems*, *14*(5), 758–775. doi:10.1007/s10021-011-9444-8

Meigs, G. W., Zald, H. S. J., Campbell, J. L., Keeton, W. S., & Kennedy, R. E. (2016). Do insect outbreaks reduce the severity of subsequent forest fires? *Environmental Research Letters*, *11*(4), 1–10. doi:10.1088/1748-9326/11/4/045008

Miller, J. D., Knapp, E. E., Key, C. H., Skinner, C. N., Isbell, C. J., Creasy, R. M., & Sherlock, J. W. (2009). Calibration and validation of the relative differenced Normalized Burn Ratio (RdNBR) to three measures of fire severity in the Sierra Nevada and Klamath Mountains, California, USA. *Remote Sensing of Environment*, *113*(3), 645–656. doi:10.1016/j.rse.2008.11.009

Miller, J. D., & Quayle, B. (2015). Calibration an Validation of Immediate Post-Fire Satellite-Derived Data to Three Severity Metrics. *Fire Ecology*, *62*(4), 789–798. doi:10.4996/fireecology.1102012

Miller, J. D., Safford, H. D., Crimmins, M., & Thode, A. E. (2009). Quantitative Evidence for Increasing Forest Fire Severity in the Sierra Nevada and Southern Cascade Mountains, California and Nevada, USA. *Ecosystems*, *12*(1), 16–32. doi:10.1007/s10021-008-9201-9

Miller, J. D., & Thode, A. E. (2007). Quantifying burn severity in a heterogeneous landscape with a relative version of the delta Normalized Burn Ratio (dNBR). *Remote Sensing of Environment*, *109*(1), 66–80. doi:10.1016/j.rse.2006.12.006

Miller, J. D., & Yool, S. R. (2002). Mapping forest post-fire canopy consumption in several overstory types using multi-temporal Landsat TM and ETM data. *Remote Sensing of Environment*, *82*(2-3), 481–496. doi:10.1016/S0034-4257(02)00071-8

Moghaddas, J. J., & Craggs, L. (2007). A fuel treatment reduces fire severity and increases suppression efficiency in a mixed conifer forest. *International Journal of Wildland Fire*, *16*(6), 673–678. doi:10.1071/WF06066

Moody, J. A., Martin, D. A., Haire, S. L., & Kinner, D. A. (2008). Linking runoff response to burn severity after a wildfire. *Hydrological Processes*, *22*(13), 2063–2074. doi:10.1002/hyp.6806

Morgan, P., Keane, R. E., Dillon, G. K., Jain, T. B., Hudak, A. T., Karau, E. C., … Strand, E. K. (2014). Challenges of assessing fire and burn severity using field measures, remote sensing and modelling. *International Journal of Wildland Fire*, *23*(8), 1045. doi:10.1071/WF13058

Moritz, M. A., Parisien, M.-A., Batllori, E., Krawchuk, M. A., Van Dorn, J., Ganz, D. J., & Hayhoe, K. (2012). Climate change and disruptions to global fire activity. *Ecosphere*, *3*(6), 1–22. doi:10.1890/ES11-00345.1

Muggeo, V. M. R. (2008). segmented: An R Package to Fit Regression Models with Broken-Line Relationships. Retrieved April 21, 2016, from https://cran.r-project.org/doc/Rnews/

Nagelkerke, N. J. D. (1991). A note on a general definition of the coefficient of determination. *Biometrika*, *78*(3), 691–692. doi:10.1093/biomet/78.3.691

Pace, R. K., & LeSage, J. P. (2004). Chebyshev approximation of log-determinants of spatial weight matrices. *Computational Statistics and Data Analysis*, *45*(2), 179–196. doi:10.1016/S0167-9473(02)00321-3

Page, W. G., & Jenkins, M. J. (2007). Predicted fire behavior in selected mountain pine beetle infested lodgepole pine. *Forest Science*, *53*(6), 662–674. Retrieved from http://www.ingentaconnect.com/content/saf/fs/2007/00000053/00000006/art00006

Parks, S., Dillon, G., & Miller, C. (2014). A New Metric for Quantifying Burn Severity: The Relativized Burn Ratio. *Remote Sensing*, *6*(3), 1827–1844. doi:10.3390/rs6031827

Patterson, M. W., & Yool, S. R. (1998). Mapping Fire-Induced Vegetation Mortality Using Landsat Thematic Mapper Data. *Remote Sensing of Environment*, *65*(2), 132–142. doi:10.1016/S0034-4257(98)00018-2

Pollet, J., & Omi, P. N. (2002). Effect of thinning and prescribed burning on crown fire severity in ponderosa pine forests. *International Journal of Wildland Fire*, *11*, 1–10.

Prichard, S. J., & Kennedy, M. C. (2014). Fuel treatments and landform modify landscape patterns of burn severity in an extreme fire event. *Ecological Applications*, *24*(3), 571–590. doi:10.1890/13-0343.1

Prichard, S. J., Peterson, D. L., & Jacobson, K. (2010). Fuel treatments reduce the severity of wildfire effects in dry mixed conifer forest, Washington, USA. *Canadian Journal of Forest Research*, *40*(8), 1615–1626. doi:10.1139/X10-109

R Development Core Team. (2014). A language and environment for statistical computing. Vienna, Austria: R Foundation for Statistical Computing. Retrieved from https://www.r-project.org/

Raffa, K. F., Aukema, B. H., Bentz, B. J., Carroll, A. L., Hicke, J. A., Turner, M. G., & Romme, W. H. (2008). Cross-scale Drivers of Natural Disturbances Prone to Anthropogenic Amplification: The Dynamics of Bark Beetle Eruptions. *BioScience*, *58*(6), 501–517. doi:10.1641/B580607

Randerson, J. T., Chen, Y., van der Werf, G. R., Rogers, B. M., & Morton, D. C. (2012). Global burned area and biomass burning emissions from small fires. *Journal of Geophysical Research: Biogeosciences*, *117*(4). doi:10.1029/2012JG002128

Raymond, C. L., & Peterson, D. L. (2005). Fuel treatments alter the effects of wildfire in a mixed-evergreen forest, Oregon, USA. *Canadian Journal of Forest Research*, *35*(12), 2981–2995. doi:10.1139/x05-206

Reddy, A. D., Hawbaker, T. J., Wurster, F., Zhu, Z., Ward, S., Newcomb, D., & Murray, R. (2015). Quantifying soil carbon loss and uncertainty from a peatland wildfire using multi-temporal LiDAR. *Remote Sensing of Environment*, *170*, 306–316. doi:10.1016/j.rse.2015.09.017

Ritchie, M. W., Skinner, C. N., & Hamilton, T. A. (2007). Probability of tree survival after wildfire in an interior pine forest of northern California: Effects of thinning and prescribed fire. *Forest Ecology and Management*, *247*(1-3), 200–208. doi:10.1016/j.foreco.2007.04.044

Robichaud, P. R., Lewis, S. A., Brown, R. E., & Ashmun, L. E. (2009). Emergency Post-fire Rehabilitation Treatment Effects on Burned Area Ecology and Long-term Restoration. *Fire Ecology Special Issue*, *5*(1), 115–128.

Rogan, J., & Yool, S. (2001). Mapping fire-induced vegetation depletion in the Peloncillo Mountains, Arizona and New Mexico. *International Journal of Remote Sensing*, *22*(16), 3101–3121. doi:10.1080/01431160152558279

Romme, W. H., Boyce, M. S., Gresswell, R., Merrill, E. H., Minshall, G. W., Whitlock, C., & Turner, M. G. (2011). Twenty Years After the 1988 Yellowstone Fires: Lessons About Disturbance and Ecosystems. *Ecosystems*, *14*(7), 1196–1215. doi:10.1007/s10021-011-9470-6

Rouse, J. W., Haas, R. H., Deerling, D. W., Schell, J. A., & Harlan, J. C. (1974). *Monitoring the vernal advancement and retrogradation (green wave effect) of natural vegetation*. Greenbelt, MD: NASA/GSFC Type III Final Report.

Roy, D. P., Boschetti, L., & Smith, A. M. S. (2013). Satellite Remote Sensing of Fires. In C. M. Belcher & G. Rein (Eds.), *Fire Phenomena and the Earth System: an interdisciplinary guide to fire science* (pp. 77–93). Oxford: John Wiley & Sons. doi:10.1002/9781118529539.ch5

Roy, D. P., Boschetti, L., & Trigg, S. N. (2006). Remote Sensing of Fire Severity: Assessing the Performance of the Normalized Burn Ratio. *IEEE Geoscience and Remote Sensing Letters*, *3*(1), 112–116. doi:10.1109/LGRS.2005.858485

Safford, H. D., Schmidt, D. A., & Carlson, C. H. (2009). Effects of fuel treatments on fire severity in an area of wildland-urban interface, Angora Fire, Lake Tahoe Basin, California. *Forest Ecology and Management, 258*(5), 773–787. doi:10.1016/j.foreco.2009.05.024

Safford, H. D., Stevens, J. T., Merriam, K., Meyer, M. D., & Latimer, A. M. (2012). Fuel treatment effectiveness in California yellow pine and mixed conifer forests. *Forest Ecology and Management, 274*, 17–28. doi:10.1016/j.foreco.2012.02.013

Schoennagel, T., Veblen, T. T., Negron, J. F., & Smith, J. M. (2012). Effects of mountain pine beetle on fuels and expected fire behavior in lodgepole pine forests, Colorado, USA. *PLoS ONE*, *7*(1), 1–14. doi:10.1371/journal.pone.0030002

Seielstad, C. A., & Queen, L. P. (2003). Using airborne laser altimetry to determine fuel models for estimating fire behaviour. *Journal of Forestry*, *101*(4), 10–15.

Simard, M., Romme, W. H., Griffin, J. M., & Turner, M. G. (2011). Do mountain pine beetle outbreaks change the probability of active crown fire in lodgepole pine forests? *Ecological Monographs*, *81*(1), 3–24. doi:10.1890/10-1176.1

Skowronski, N. S., Clark, K. L., Gallagher, M., Birdsey, R. A., & Hom, J. L. (2014). Airborne laser scanner-assisted estimation of aboveground biomass change in a temperate oak-pine forest. *Remote Sensing of Environment*, *151*, 166–174. doi:10.1016/j.rse.2013.12.015

Smith, A. M. S., Drake, N. A., Wooster, M. J., Hudak, A. T., Holden, Z. A., & Gibbons, C. J. (2007). Production of Landsat ETM+ reference imagery of burned areas within Southern African savannahs: comparison of methods and application to MODIS. *International Journal of Remote Sensing*, *28*(12), 2753–2775. doi:10.1080/01431160600954704

Smith, A. M. S., Eitel, J. U. H., & Hudak, A. T. (2010). Spectral analysis of charcoal on soils: Implicationsfor wildland fire severity mapping methods. *International Journal of Wildland Fire*, *19*(7), 976–983. doi:10.1071/WF09057

Smith, A. M. S., Falkowski, M. J., Hudak, A. T., Evans, J. S., Robinson, A. P., & Steele, C. M. (2009). A cross-comparison of field, spectral, and lidar estimates of forest canopy cover. *Canadian Journal of Remote Sensing*, *35*(5), 447–459. doi:10.5589/m09-038

Smith, A. M. S., Kolden, C. A., Tinkham, W. T., Talhelm, A. F., Marshall, J. D., Hudak, A. T., … Gosz, J. R. (2014). Remote sensing the vulnerability of vegetation in natural terrestrial ecosystems. *Remote Sensing of Environment, 154*, 322–337. doi:10.1016/j.rse.2014.03.038

Smith, A. M. S., Sparks, A. M., Kolden, C. A., Abatzoglou, J. T., Talhelm, A. F., Johnson, D. M., … Kremens, R. J. (2016). Towards a new paradigm in fire severity research using dose–response experiments. *International Journal of Wildland Fire*, *25*(2), 158–166. doi:10.1071/WF15130

Sparks, A. M., Boschetti, L., Smith, A. M. S., Tinkham, W. T., Lannom, K. O., & Newingham, B. A. (2015). An accuracy assessment of the MTBS burned area product for shrub–steppe fires in the northern Great Basin, United States. *International Journal of Wildland Fire*, *24*(1), 70. doi:10.1071/WF14131

Stephens, S. L., Collins, B. M., & Roller, G. (2012). Fuel treatment longevity in a Sierra Nevada

mixed conifer forest. *Forest Ecology and Management*, *285*, 204–212. doi:10.1016/j.foreco.2012.08.030

Stephens, S. L., & Moghaddas, J. J. (2005). Experimental fuel treatment impacts on forest structure, potential fire behavior, and predicted tree mortality in a California mixed conifer forest. *Forest Ecology and Management*, *215*(1-3), 21–36. doi:10.1016/j.foreco.2005.03.070

Stephens, S. L., Moghaddas, J. J., Edminster, C., Fiedler, C. E., Haase, S., Harrington, M., … Youngblood, A. (2009). Fire Treatment Effects on Vegetation Structure , Fuels , and Potential Fire Severity in Western U . S . Forests. *Ecological Applications*, *19*(2), 305–320. doi:10.1890/07-1755.1

Strom, B. A., & Fulé, P. Z. (2007). Pre-wildfire fuel treatments affect long-term ponderosa pine forest dynamics. *International Journal of Wildland Fire*, *16*(1), 128–138. doi:10.1071/WF06051

Thompson, J. R., Spies, T. A., & Ganio, L. M. (2007). Reburn severity in managed and unmanaged vegetation in a large wildfire. *Proceedings of the National Academy of Sciences of the United States of America*, *104*(25), 10743–8. doi:10.1073/pnas.0700229104

Tinkham, W. T., Smith, A. M. S., Marshall, H. P., Link, T. E., Falkowski, M. J., & Winstral, A. H. (2014). Quantifying spatial distribution of snow depth errors from LiDAR using Random Forest. *Remote Sensing of Environment*, *141*, 105–115. doi:10.1016/j.rse.2013.10.021

Trigg, S., & Flasse, S. (2001). An evaluation of different bi-spectral spaces for discriminating burned shrub-savannah. *International Journal of Remote Sensing*, *22*(13), 2641–2647. doi:10.1080/01431160110053185

Turner, M. G., Hargrove, W. W., Gardner, R. H., & Romme, W. H. (1994). Effects of Fire on Landscape Heterogeneity in Yellowstone National Park , Wyoming. *Journal of Vegetation Science*, *5*(5), 731–742.

Turner, M. G., Romme, W. H., & Gardner, R. H. (1999). Prefire heterogeneity, fire severity, and early postfire plant reestablishment in subalpine forests of Yellowstone National Park, Wyoming. *International Journal Of Wildland Fire*, *9*(1), 21–36. doi:doi:10.1071/WF99003

van Leeuwen, W. J. D. (2008). Monitoring the Effects of Forest Restoration Treatments on Post-Fire Vegetation Recovery with MODIS Multitemporal Data. *Sensors*, *8*(3), 2017–2042. doi:10.3390/s8032017

van Wagtendonk, J. W. (1996). Use of a Deterministic Fire Growth Model to Test Fuel Treatments. *Sierra Nevada Ecosystem Project: Final Report to Congress, Vol. II*, *II*, 1155–1166.

van Wagtendonk, J. W., Root, R. R., & Key, C. H. (2004). Comparison of AVIRIS and Landsat ETM+ detection capabilities for burn severity. *Remote Sensing of Environment*, *92*(3), 397–408. doi:10.1016/j.rse.2003.12.015

Wang, C., & Glenn, N. F. (2009). Estimation of fire severity using pre- and post-fire LiDAR data in sagebrush steppe rangelands. *International Journal of Wildland Fire*, *18*(7), 848–856. doi:10.1071/WF08173

Westerling, A. L., Hidalgo, H. G., Cayan, D. R., & Swetnam, T. W. (2006). Warming and earlier spring increase western U.S. forest wildfire activity. *Science*, *313*(5789), 940–943. doi:10.1126/science.1128834

White, J. D., Ryan, K. C., Key, C. C., & Running, S. W. (1996). Remote Sensing of Forest Fire Severity and Vegetation Recovery. *International Journal of Wildland Fire*, *6*(3), 125–136.

Whittier, T. R., & Gray, A. N. (2016). Tree mortality based fire severity classification for forest inventories: A Pacific Northwest national forests example. *Forest Ecology and Management*, *359*, 199–209. doi:10.1016/j.foreco.2015.10.015

Wimberly, M. C., Cochrane, M. A., Baer, A. D., & Pabst, K. (2009). Assessing fuel treatment effectivness using satellite imagery and spatial statistics. *Ecological Applications*, *19*(6), 1377–1384. Retrieved from http://www.jstor.org/stable/40346253

Wimberly, M. C., & Reilly, M. (2007). Assessment of fire severity and species diversity in the southern Appalachians using Landsat TM and ETM+ imagery. *Remote Sensing of Environment*, *108*(2), 189–197. doi:10.1016/j.rse.2006.03.019

Wing, B. M., Ritchie, M. W., Boston, K., Cohen, W. B., Gitelman, A., & Olsen, M. J. (2012). Prediction of understory vegetation cover with airborne lidar in an interior ponderosa pine forest. *Remote Sensing of Environment*, *124*, 730–741. doi:10.1016/j.rse.2012.06.024

Wing, B. M., Ritchie, M. W., Boston, K., Cohen, W. B., & Olsen, M. J. (2015). Individual snag detection using neighborhood attribute filtered airborne lidar data. *Remote Sensing of Environment*, *163*, 165–179. doi:10.1016/j.rse.2015.03.013

Wulder, M. A., White, J. C., Alvarez, F., Han, T., Rogan, J., & Hawkes, B. (2009). Characterizing boreal forest wildfire with multi-temporal Landsat and LIDAR data. *Remote Sensing of Environment*, *113*(7), 1540–1555. doi:10.1016/j.rse.2009.03.004

Zhu, Z., Key, C. H., Ohlen, D., & Benson, N. (2006). *Mapping Algorithms for Different Ecosystems*. Final Report to the Joint Fire Science Program.

Appendix A: Coefficients for Principle Component Analysis

Delta Principle Component 1 (dPC1)	(dB*0.6052) + (dG*0.5723) + (dR*0.7756) + (dNIR*-0.6761) + (dSWIR1*0.8943) + (dSWIR2*0.9720)
Delta Principle Component 2 (dPC2)	(dB*0.3909) + (dG*0.5048) + (dR*0.2976) + (dNIR*0.7287) + (dSWIR1*0.2863) + (dSWIR2*0.0659)
Delta Principle Component 3 (dPC3)	(dB*0.3339) + (dG*0.4090) + (dR*0.2748) + (dNIR*0.0438) + (dSWIR1*-0.3401) + (dSWIR2*0.1592)

Coefficients applied to differenced Landsat Bands (Blue (dB), Green (dG), Red (dR), Near Infrared (dNIR), Shortwave Infrared 1 (dSWIR1), and Shortwave Infrared 2 (dSWIR2))

Appendix B: Pearson's Correlation Coefficients for all Model Combinations

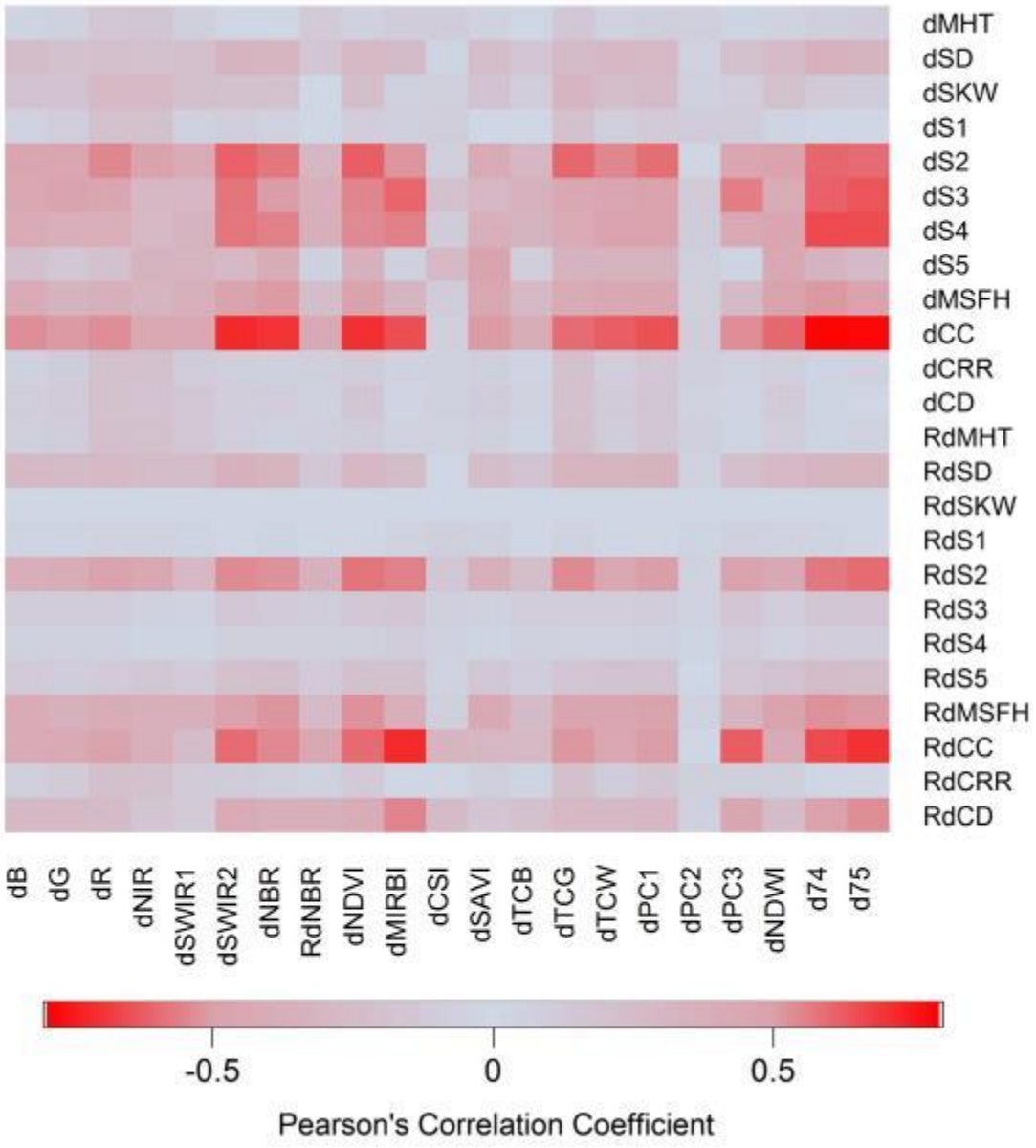

Acronyms defined in Table 1.2 and 1.3.

Appendix C: Average MPB Mortality 1993-2012

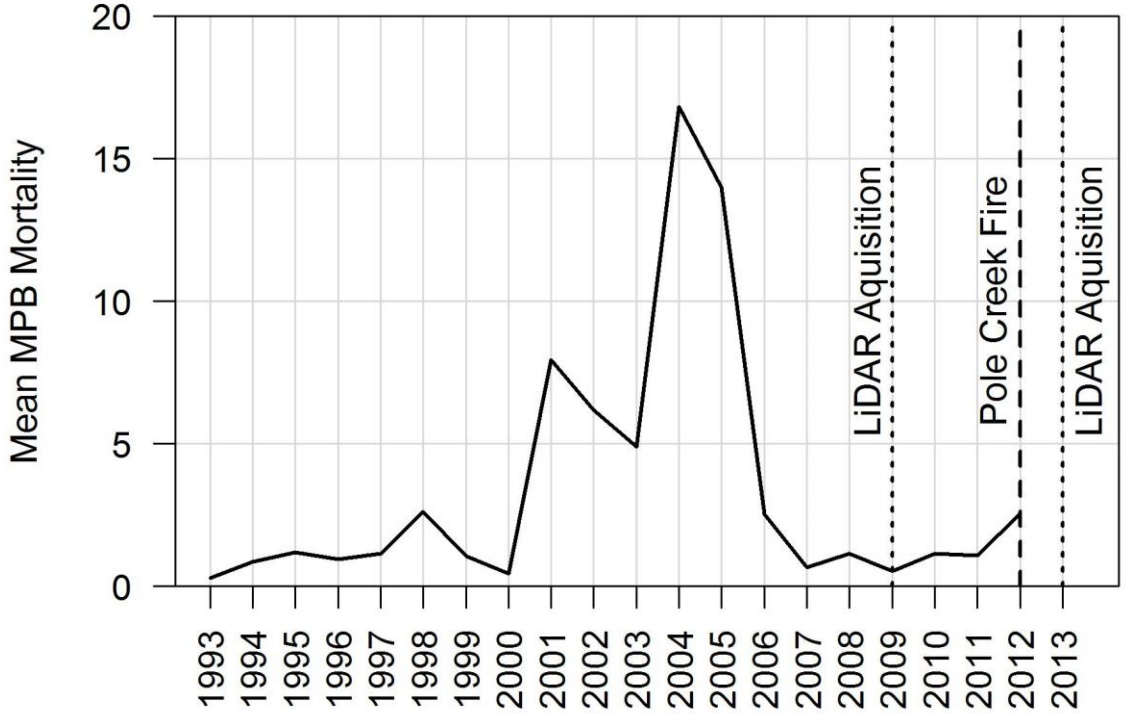

Average mountain pine beetle (MPB) induced mortality from 1993 until the fire (2012) across the area of LiDAR acquisition affected by MPB; peak mortality occurs between 2000 and 2006.

Appendix D: Model R-squares in Fire-only Areas at Different MPB Levels

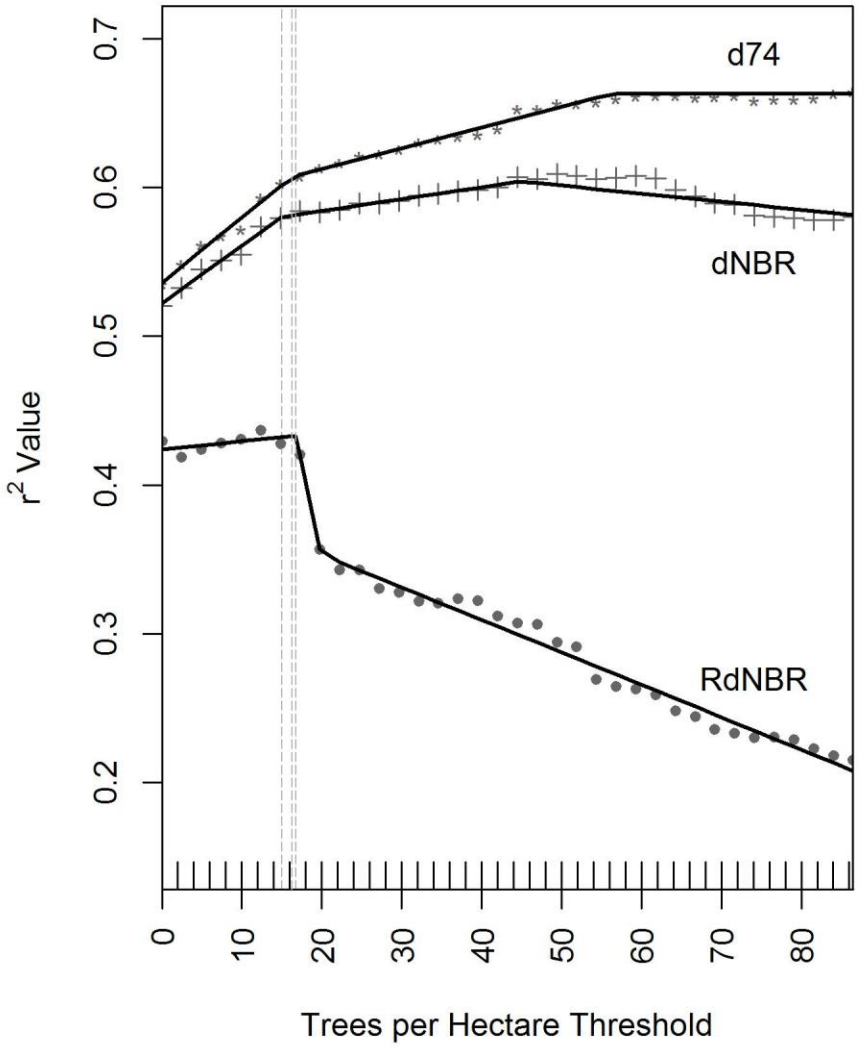

Model r-squared values for pixels not experiencing either mountain pine beetle (MPB) or forest treatment using different thresholds of MPB. Vertical lines represent breakpoints calculated by the iterative procedure, indicating thresholds where increasing MPB intensity changes the model (approximately 16 trees per hectare). Spectral indices (delta band 7/4 ratio, d74; delta normalized burn ratio, dNBR; and relative dNBR, RdNBR) are regressed on percent canopy cover change using the best linear fit.